TÜBİTAK

Turkish Journal of Earth Sciences

http://journals.tubitak.gov.tr/earth/

Research Article

Turkish J Earth Sci
(2023) 32: 1-26
© TÜBİTAK
doi:10.55730/1300-0985.1825

Calcareous nannofossils, planktonic foraminifera, and revised stratigraphy of the Eocene Çayraz Formation; the final stage of marine sedimentation in Central Anatolia, Turkey

Ali Osman YÜCEL[1,*], Ercan ÖZCAN[1,♀], Rita CATANZARITI[2], Aynur HAKYEMEZ[3], Aral I. OKAY[1,4], Attila ÇİNER[4,5], Ali AKIN[1]

[1]Department of Geological Engineering, Faculty of Mines, İstanbul Technical University, İstanbul, Turkey
[2]Istituto di Geoscienze e Georisorse CNR, Pisa, Italy
[3]Department of Geological Research, General Directorate of Mineral Research and Exploration, Ankara, Turkey
[4]Eurasia Institute of Earth Sciences, İstanbul Technical University, İstanbul, Turkey
[5]Department of Geography, Universidad de Barcelona, Barcelona, Spain

Received: 23.07.2022 • **Accepted/Published Online:** 03.12.2022 • **Final Version:** 19.01.2023

Abstract: New field observations and discovery of calcareous nannofossils and planktonic foraminifera from the 'shallow-marine' Çayraz Formation (Haymana Basin, Central Anatolia), a contributing Eocene section to the shallow benthic zonation (SBZ) in the Tethys, allow us to revise its stratigraphy and establish an integrated biostratigraphic scheme for the first time. The hemipelagic marls in the uppermost part of the Eskipolatlı Formation that underlies the Çayraz Formation yielded nannofossil assemblages of Zone CNE3, pinning down the initiation of the Çayraz shelf system into the 'middle' Ypresian. The prominent marly part (Member B) between the carbonate-clastic packages of the Çayraz Formation with prolific occurrences of larger benthic foraminifers (LBFs) (Members A below and C above) yielded calcareous nannofossils suggesting Zone CNE6 (late Ypresian). We show that the mixed carbonate-siliciclastic sequence with abundant LBFs in the upper part of the formation (Member C) is overlain by newly discovered hemipelagic marls (here named as Member D). These marls yielded calcareous nannofossils indicating Zone CNE9 and CNE10 for the lower and Zone CNE12(?Lutetian) for the upper samples. The same beds yielded planktonic foraminifers indicating Zone E8 for the lower and Zone E9 for the upper samples. We conclude that shallow-marine sedimentation in the Çayraz section ended in the 'middle' Lutetian, challenging the previous Bartonian records by LBFs. A new lithostratigraphic scheme consisting of four members with distinctive lithological and biotic characteristics is proposed for the Çayraz Formation: two main shelf systems (Members A and C), each followed by deep-marine sedimentation (Members B and D).

Key words: Çayraz Formation, Eskipolatlı Formation, calcareous nannofossils, planktonic foraminifera, Eocene, Haymana Basin

1. Introduction

The Çayraz Formation in Central Anatolia is exceptional, being one of the most continuous Eocene ('middle' Ypresian to middle Eocene) successions with prolific accumulations of larger benthic foraminifers (LBFs). It constitutes a crucial contributing section to the currently widely used shallow benthic zonation of the Paleogene (Serra-Kiel et al., 1998, Papazzoni et al., 2017). This unit, well exposed near Çayraz village in the Haymana Basin southwest of Ankara, is characterized by a mixed carbonate-siliciclastic sequence (>350 m in thickness), recording the final stage of the Cenozoic marine sedimentation in Central Anatolia (Ünalan et al., 1976; Sirel, 1992; Çiner et al., 1996a; Özcan, 2002; Özcan et al., 2018, 2020; Okay et al., 2020) (Figures 1, 2A, 3A–3C). The Çayraz profile includes about 10 million years of continuous stratigraphic record and almost continuous occurrences of LBFs (Figure 4). The Çayraz Formation was long interpreted as an 'undifferentiated' shallow-marine sequence deposited in a foredeep setting along the south-facing active margin of Eurasia during the Eocene (Ünalan et al., 1976; Koçyiğit, 1991; Sirel, 1992; Çiner et al., 1996a; Özcan, 2002; Okay and Altıner, 2016). This concept was, however, lately challenged by Özcan et al. (2020), showing that the middle marly beds of the Çayraz Formation (Member B in this study, Figures 2A, 5C–5D) contain abundant planktonic foraminifera (indicative of P9 Zone= E7 Zone) suggesting an environmental turnover across the Ypresian-Lutetian boundary. Özcan et al. (2020) subdivided

♀ This paper is dedicated to the late Ercan Özcan, who left us in December 2022, for his tremendous contributions to the paleontology of the larger benthic foraminifera.

* Correspondence: aliosmanyucel@gmail.com

This work is licensed under a Creative Commons Attribution 4.0 International License.

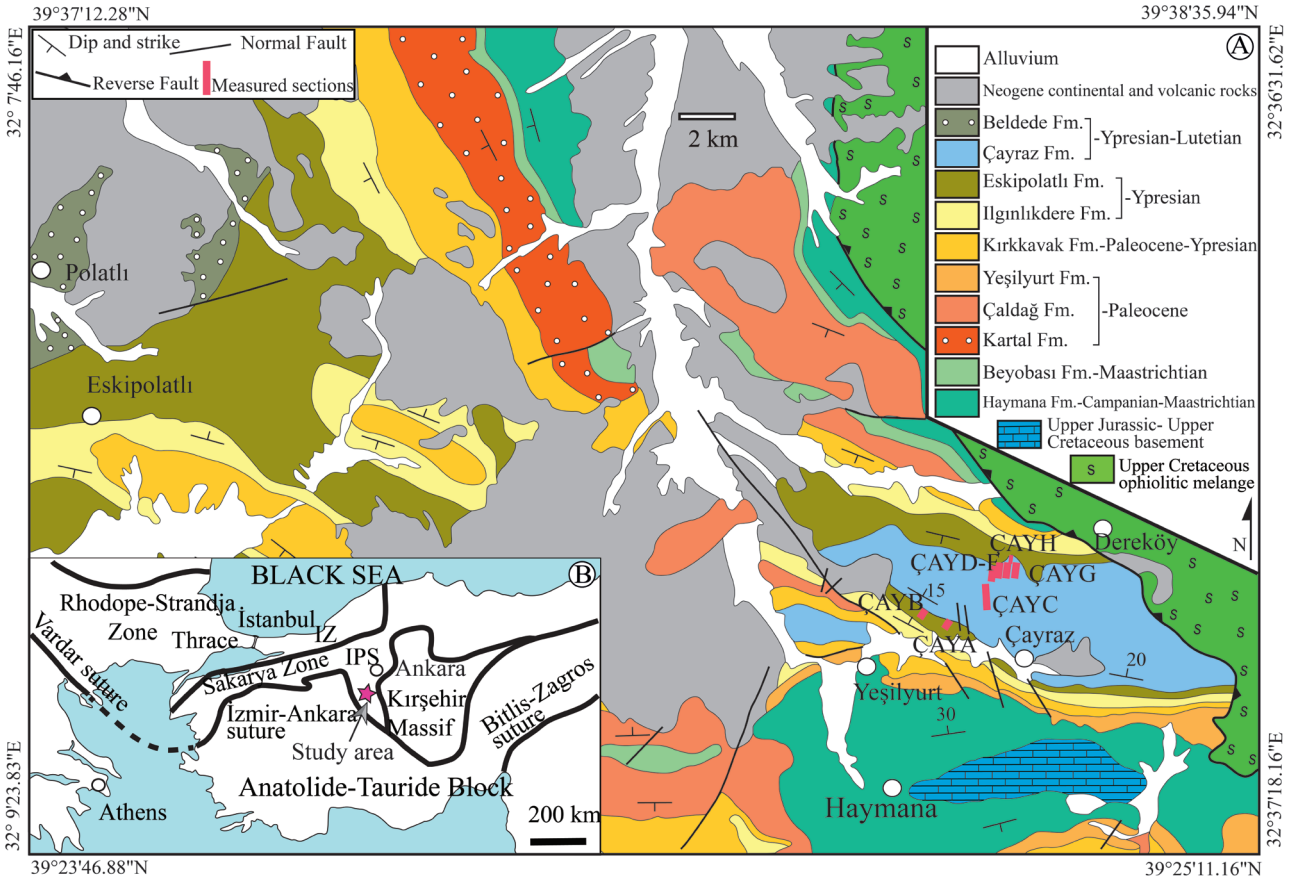

Figure 1. A) Geological map of the Haymana region southwest of Ankara with the locations of the sections studied, **B)** Tectonic map of Turkey showing the major sutures and continental blocks (tectonic map simplified from Okay and Tüysüz, 1999 and geological map of the Haymana-Polatlı region after Ünalan et al., 1976). IZ: Istanbul Zone, IPS: Intra-Pontid Suture.

the Çayraz Formation into three lithologically distinct units at its type area near Çayraz village: the lower (approximately 100–110-m-thick) and upper (approximately 152-m-thick) units being represented by mixed carbonate-siliciclastic sequence with abundant LBFs (Figures 5A, 5B, 5E, and 5F) and the middle unit (approximately 50-m-thick) by massive marl-siltstone beds barren in LBFs (Figure 5C and 5D), but moderately abundant planktonic foraminifera suggesting deepening of the depositional environment across the Ypresian-Lutetian boundary (Özcan et al., 2020). The previous studies concluded that the marine sedimentation in the region ended with the deposition of the upper mixed carbonate-siliciclastic section (Member C in this study) with abundant LBFs, which are believed to be unconformably overlain by Neogene-Quaternary terrestrial or volcanic rocks (Ünalan et al., 1976; Sirel and Deveciler, 2017; Özcan et al., 2020; Okay et al., 2020).

This paper aims to resolve the pending issues outlined below:

1- The initiation of the shallow marine sedimentation of the Çayraz Formation (Member A) was interpreted to have occurred either in the Ypresian or in the Lutetian (Table 1 and also see Toker, 1980). Until now, except for Member B, which was recently studied for planktonic foraminifera (Özcan et al., 2020), all age assignments relied on the study of LBFs. Therefore, a necessity for an integrated biostratigraphy of various fossil groups has arisen. The upper part of the underlying Eskipolatlı Formation consisting of deep-marine siliciclastic beds would potentially provide the most appropriate data for the onset of shallow-marine sedimentation of the Çayraz Formation (Figures 2A and 4).

2- A detailed study of Member B, pelagic marly-silty unit topping Member A, would provide information to constrain the upper age limit of Member A and transition to the pelagic sedimentation in the Çayraz section (Figures 2A and 4). The data previously provided by the planktonic foraminifera (indicative of P9 Zone) suggest that this event occurred across the Ypresian-Lutetian boundary (Özcan et al., 2020). However, this requires a further study of calcareous nannofossils which provides an integrated biostratigraphic scheme.

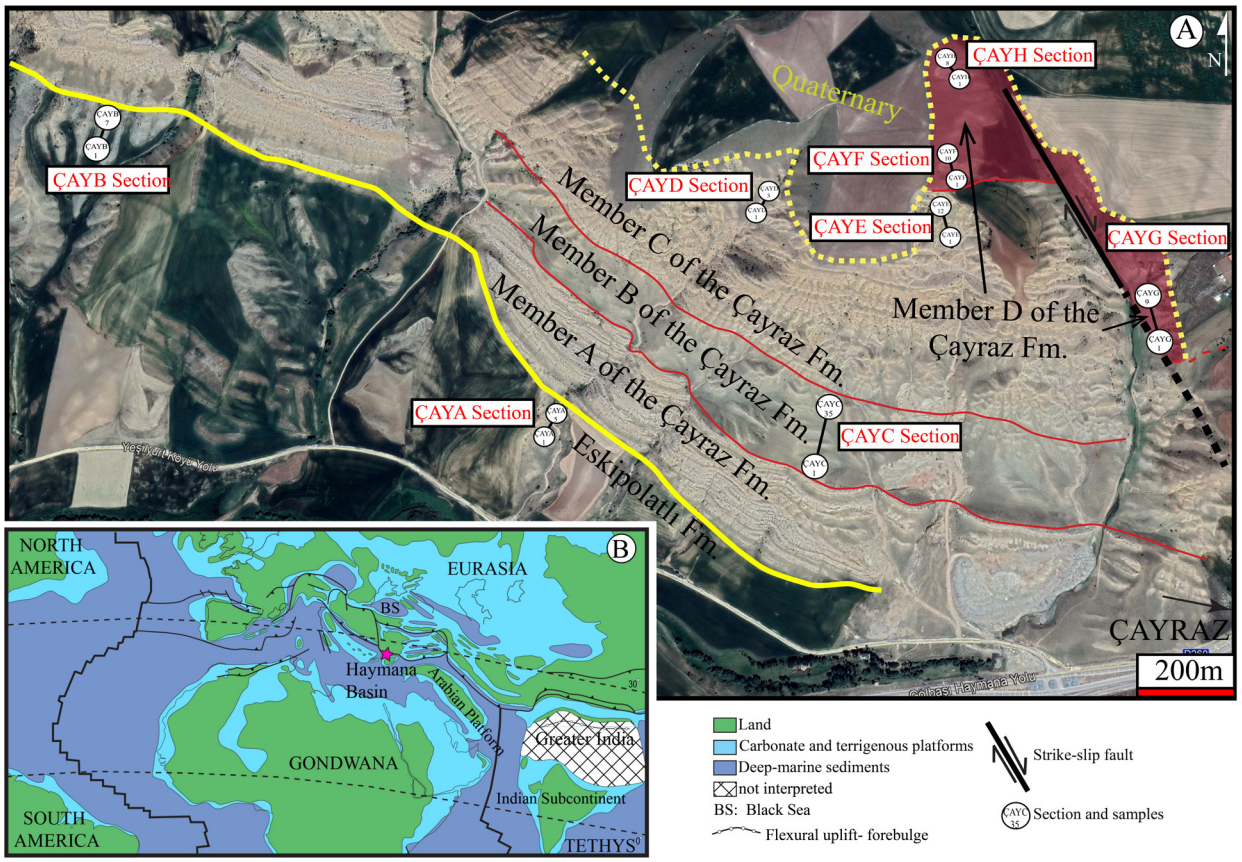

Figure 2. A) Aerial photograph of the Çayraz region, showing the positions of the studied sections from the Eskipolatlı and Çayraz formations. **B)** Paleogeographic position of Haymana Basin in the Eocene. BS: Black Sea.

3- Termination age of the shallow marine sedimentation (Member C), previously recorded only by LBFs, needs precision since age assignments are various, either referred to (middle) Lutetian or Bartonian (Table 1) and far from a high-resolution perspective. Member C is overlain by a deep-marine marly section (Member D), not reported in the previous studies. Member D, devoid of LBFs (Figures 5G–5J), forms the highest stratigraphic levels of the Çayraz Formation and exposes in a limited area on the N-S running creeks near Çayraz village along an NW-SE running fault (Figure 2A). Since the Çayraz Formation was believed to have ended with nummulitic beds, a study of Member D for calcareous nannoplanktons and planktonic foraminifera is of utmost importance for high-resolution biostratigraphy and to better constrain the transition from marine to the continental environment in Central Anatolia.

2. Geological setting and regional stratigraphy

The Haymana-Polatlı Basin in Central Anatolia is an accretionary forearc to foredeep basin formed by the closure of the Neotethys during the Late Cretaceous to middle Eocene time interval (Koçyiğit et al., 1991; Okay and Altıner, 2016). The basin is close to the suture zone between Anatolide-Tauride Block/Kırşehir Massif and Sakarya Zone (Figure 1B). Basin-fill deposits ranging in age from Late Cretaceous to Eocene are represented by approximately 5-km-thick siliciclastics and fossiliferous carbonates deposited in continental to shallow- to deep-marine environments (Ünalan et al., 1976; Sirel, 1992, 1998, 1999, 2009; Sirel and Gündüz, 1976; Özcan, 2002; Özcan et al., 2007, 2001, 2020; Okay and Altıner, 2016). The palaeogeographic location of the Haymana Basin (Figure 2B) lies along the pathway between Central Tethys and Europe. The Paleocene and Eocene sequence of the Haymana Basin is characterized predominantly by siliciclastics and carbonates deposited in various environments ranging from continental to deep marine settings (Sirel, 1975; Ünalan et al., 1976). Paleocene deposits are represented by continental clastics (Kartal Formation), shallow marine limestone (Çaldağ Formation), and deep marine shales (Yeşilyurt Formation) (Ünalan et al., 1976) (Figure 1A). The upper Paleocene-lower Eocene deposits are made up of algal limestone, marl, and shale beds

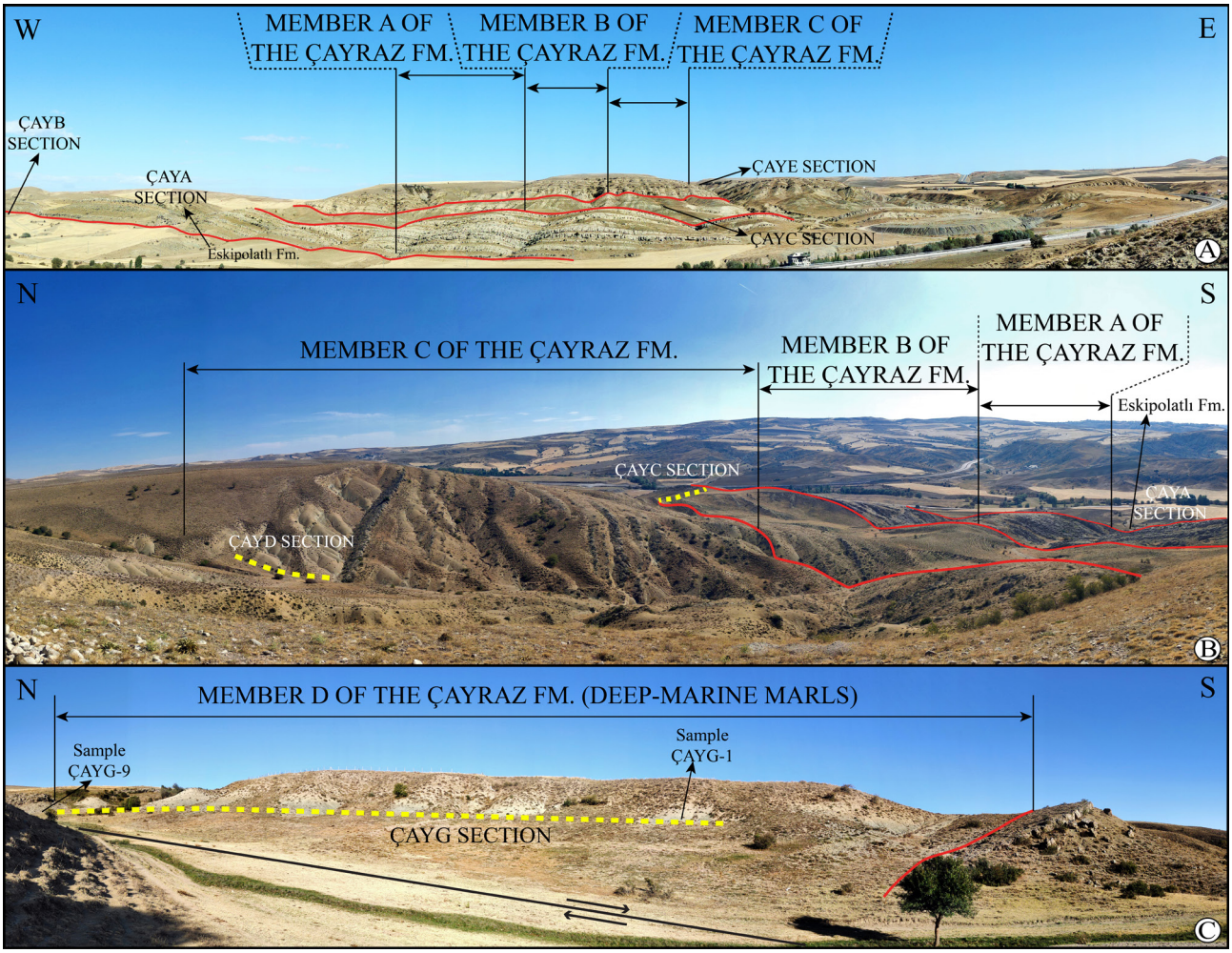

Figure 3. Field photographs of the Çayraz Formation and location of some sections. **A-B)** Panoromic views of the Çayraz Formation at its type-area near Çayraz. **C)** The marly hemipelagic succession of the Member D overlying the shallow-marine beds of the Member C in section ÇAYG.

(Kırkkavak Formation), which pass into deep marine conglomerate-sandstone-marl-shale intercalations with debris flows (Ilgınlıkdere and Eskipolatlı formations). A regional shallowing is marked by the deposition of fan delta conglomerates and sandstones (Beldede Formation) (Çiner et al., 1993), and shallow-marine Eocene Çayraz Formation (Çiner et al., 1996a; Özcan, 2002; Özcan et al., 2020), which laterally grades to the siliciclastic turbidites of the Yamak Formation (Çiner et al., 1996b). The Çayraz Formation was recently subdivided into lower and upper mixed carbonate-siliciclastic units, approximately 100- and 155-m-thick, respectively, separated by a sequence of thick-bedded to massive marl/siltstone unit, almost devoid of LBFs (herein Member B) (Özcan et al., 2020). Both lower and upper units contain densely packed LBFs in several intervals (Hottinger, 1960; Schaub, 1981; Özcan, 2002; Özcan et al., 2007, 2018; Deveciler, 2010; Sirel and Deveciler, 2017), intercalated with marly/silty interbeds, suggesting a cyclic depositional regime. The Çayraz Formation is unconformably overlain by various Neogene and Quaternary units (Figure 1).

3. Materials and methods

To the NW of the Çayraz village, a total of 84 samples were collected from eight stratigraphic sections (ÇAYA-H) (Figures 1–3). Twelve samples come from the uppermost part of the Eskipolatlı Formation (ÇAYA and B sections; Figures 2A and 4; Table 1). Thirty-five samples derive from the Member B of the Çayraz Formation (ÇAYC section; Figures 2A and 4; Table 1). This section is the same as that previously studied for planktonic foraminifera by Özcan et al. (2020). Fifteen samples come from the upper part of the Member C (respectively from ÇAYD and ÇAYE sections that are laterally equivalent and 450 m apart from each other; Figures 2A and 4; Table 1). Nineteen samples were collected from the lower part of the Member D (ÇAYF

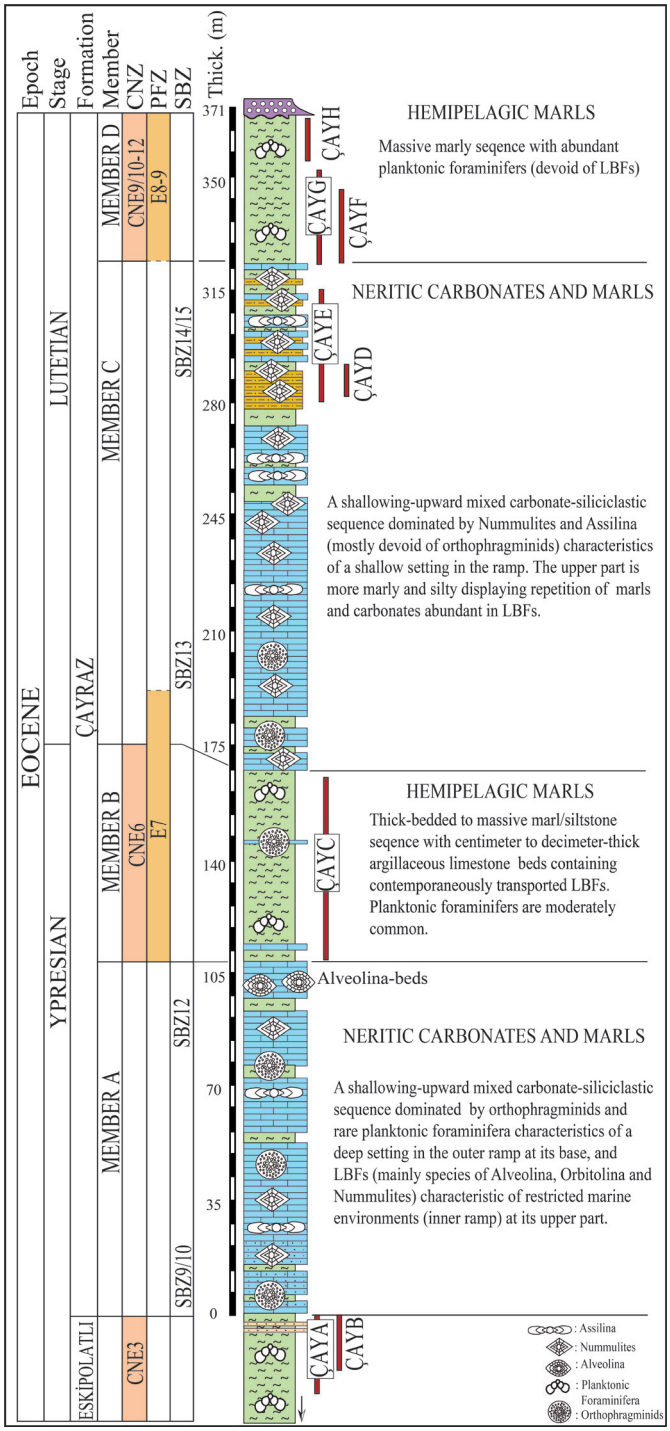

Figure 4. Generalized stratigraphic section representing the Çayraz Formation near Çayraz and proposed lithostratigraphic subdivision (Members A–D). The positions of the studied sections are shown. CNZ: calcareous nannofossil zones according to Agnini et al. (2014). SBZ: shallow-benthic zones according to Serra-Kiel et al. (1998). PFZ: planktonic foraminifera zones according to Wade et al. (2011)

and ÇAYG sections) and eight samples from its upper part (ÇAYH; Figures 2A and 4; Table 1).

Calcareous nannofossil samples were prepared as simple smear slides following standard procedures (Bown and Young, 1989). Smear slides were analyzed under a light microscope at 1250 magnification. Data were collected with semiquantitative and quantitative counting methods. Semiquantitative counting was used

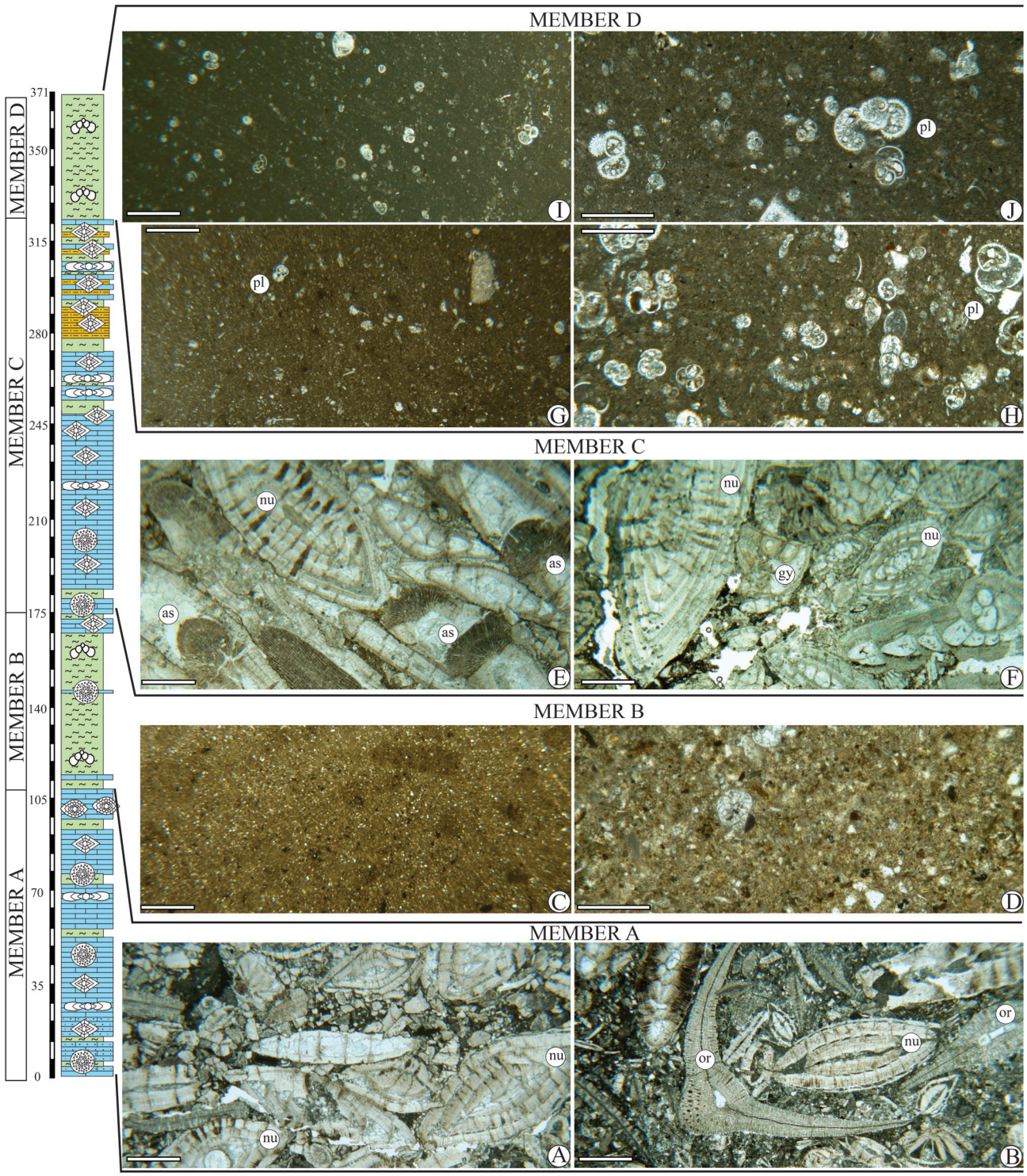

Figure 5. Photomicrographs of thin sections showing characteristic biotic features of Members A-D. **A-B)** Member A: orthophragminid-nummulitid packstone. **C-D)** Member B: planktonic foraminiferal marl, C: sample ÇAYC-12, D: sample ÇAYC-8. **E-F)** Member C: nummulitid (*Assilina* and *Nummulites*) packstone/grainstone. **G-J)** Member D: planktonic foraminiferal marl, G: sample ÇAYF-4, H: sample ÇAYH-4, I: sample ÇAYH-8, J: sample ÇAYH-3. or: orthophragminids, nu: *Nummulites*, as: *Assilina*, gy: *Gyroidinella*, pl: planktonic foraminifera. Scale bar is 500 µm.

Table 1. Previous age assignments to the Çayraz Formation.

Author(s)	***Studied levels marked with the lithostratigraphic nomenclature proposed in this study***	***Fossil groups***	***Assigned ages***
Hottinger (1960)	Member A	Alveolinids	Ypresian
Dizer (1968)	Eskipolatlı Fm., ? and Members A?, C	Nummulitids and alveolinids	Ypresian-early Lutetian
Ünalan et al. (1976)	Members A, B, C	Nummulitids and alveolinids	late Ypresian (Cuisian)-Lutetian (Upper Unit)
Sirel and Gündüz (1976)	Members A, B, C	Nummulitids and alveolinids	Ypresian (Cuisian)-Lutetian
Schaub (1981)	Member C	Nummulitids	(early) Lutetian
Özcan (2002)	Member A	Orthophragminids	SBZ 10-11/12; late Ypresian
Özcan et al. (2007)	Member B	Orthophragminids	OZ 8b (SBZ 12/13); Ypresian-Lutetian transition
	Member C	Nummulitids and orthophragminids	SBZ13-14/15; early to middle Lutetian
Deveciler (2010)	Member C	Nummulitids	Lutetian to Bartonian
Dinçer (2016)	Members A, B, C	Nummulitids	Lutetian to Bartonian
Sirel and Deveciler (2017)	Member A	Rotaliids	(late) Ypresian
Sirel and Deveciler (2018)	Members A, B, C	Nummulitids	Ypresian-Bartonian
Özcan et al., 2020	Member A	Nummulitids and orthophragminids	SBZ9/10; 'middle' Ypresian
	Member B	Planktonic foraminifera	P9 (E7); Ypresian-Lutetian transition
This study	Upper part of Eskipolatlı Fm.	Calcareous nannofossils	early-late Ypresian transition
	Member A		-
	Member B		CNE6; latest Ypresian
	Member C		-
	Member D		CNE9-12; early to middle Lutetian
	Member D	Planktonic foraminifera	E8-9; early to middle Lutetian

to record the total abundance of autochthonous and reworked nannofossils in terms of specimens per field of view (FOV); it was also used to quantify the abundance of rare species. The total abundances were reported as letters that categorize the number of specimens per field of view (N/FOV), A (Abundant, N/FOV >10), C (Common, N/FOV between 5 and 10), F (Few, N/FOV between 1 and 5), R (Rare, N/FOV <1). The abundance of rare species was reported as the number of specimens counted on 100 FOV. The quantitative counting of each species was performed on a fixed number of 300 specimens (reduced to 100 where the total abundance was rare) and reported as percentages. For *Sphenolithus* species, the counting was performed on 50 sphenoliths, only where the taxon was sufficiently abundant to satisfy this method. The occurrence of biostratigraphically significant taxa allowed the recognition of some calcareous nannofossil Eocene biozones (CNE zones of Agnini et al., 2014, NP zones of Martini, 1971 and CP zones of Okada and Bukry, 1980) useful to date the Çayraz Formation, and detailed in the biostratigraphic scheme given in Figure 6. The numerical data are reported in Appendix A (Tables S1–S8). The taxonomic list of all the cited taxa is documented in Appendix B.

Planktonic foraminifera were analyzed in the washed residues of eighteen samples collected from the sections ÇAYF and ÇAYH. The marl-siltstone samples were disaggregated by using the standard washing method of diluted hydrogen peroxide (30%) and washed using 63-, 125-, 250-μm sieves to obtain isolated specimens of

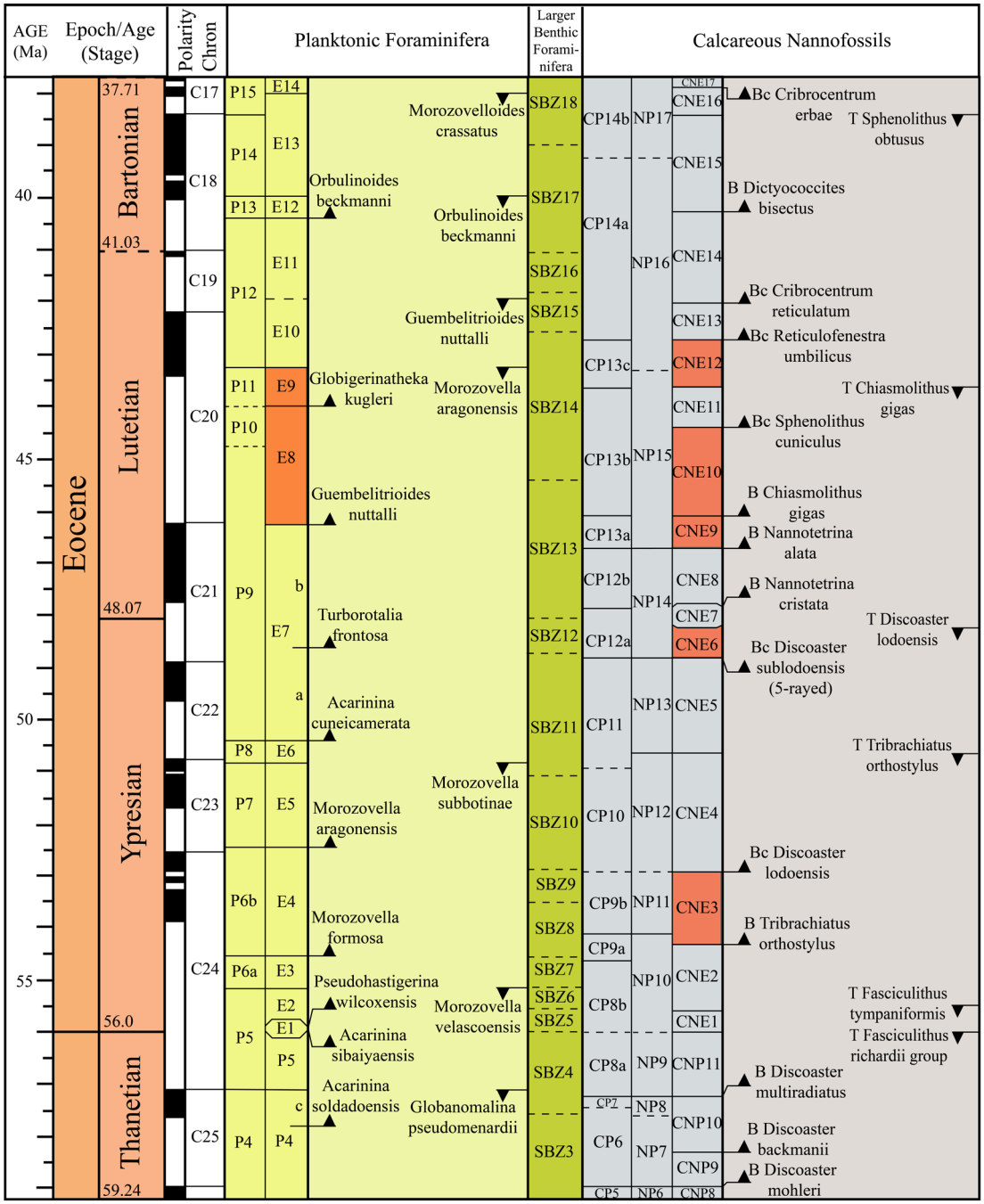

Figure 6. Correlation of calcareous nannofossil zones (CP, NP, CNE) to SBZ zones and magnetostratigraphy in Ypresian and middle Lutetian, and important datum levels of calcareous nannofossils. CP: Coccoliths Paleogene biozones according to Okada and Bukry (1980); NP: Nannoplankton Paleogene biozones according to Martini (1971); CNE: Calcareous Nannofossil Eocene biozones according to Agnini et al (2014). SBZ: Shallow Benthic Zones according to Serra-Kiel et al. (1998). Planktonic foraminifera zones according to Wade et al. (2011). Geomagnetic Polarity Time Scale according to Gradstein et al. (2012).

planktonic foraminifera. To better observe diagnostic specific characters, washed residues covered by clay particles were cleaned by boiling with Calgon solution. Photographs of selected specimens were taken by a scanning electron microscope (SEM). Taxonomic classification of planktonic foraminifera is mainly based on the "Atlas of Eocene Planktonic Foraminifera" by Pearson et al. (2006). The biozonal definition follows the standard biostratigraphic schemes of Berggren et al. (1995), Berggren and Pearson (2005) and Wade et al. (2011).

4. Results

4.1. Calcareous nannofossil biostratigraphy

The Eskipolatli Formation (Sections ÇAYA and ÇAYB, Figure 7) contains scarce and poorly preserved calcareous nannofossils, partly characterized by Cretaceous and Paleocene reworked forms. Among the autochthonous taxa, there are some specimens of *Coccolithus pelagicus* (Figure 8L) and of *Toweius* (e.g., *callosus*, *gammation* as

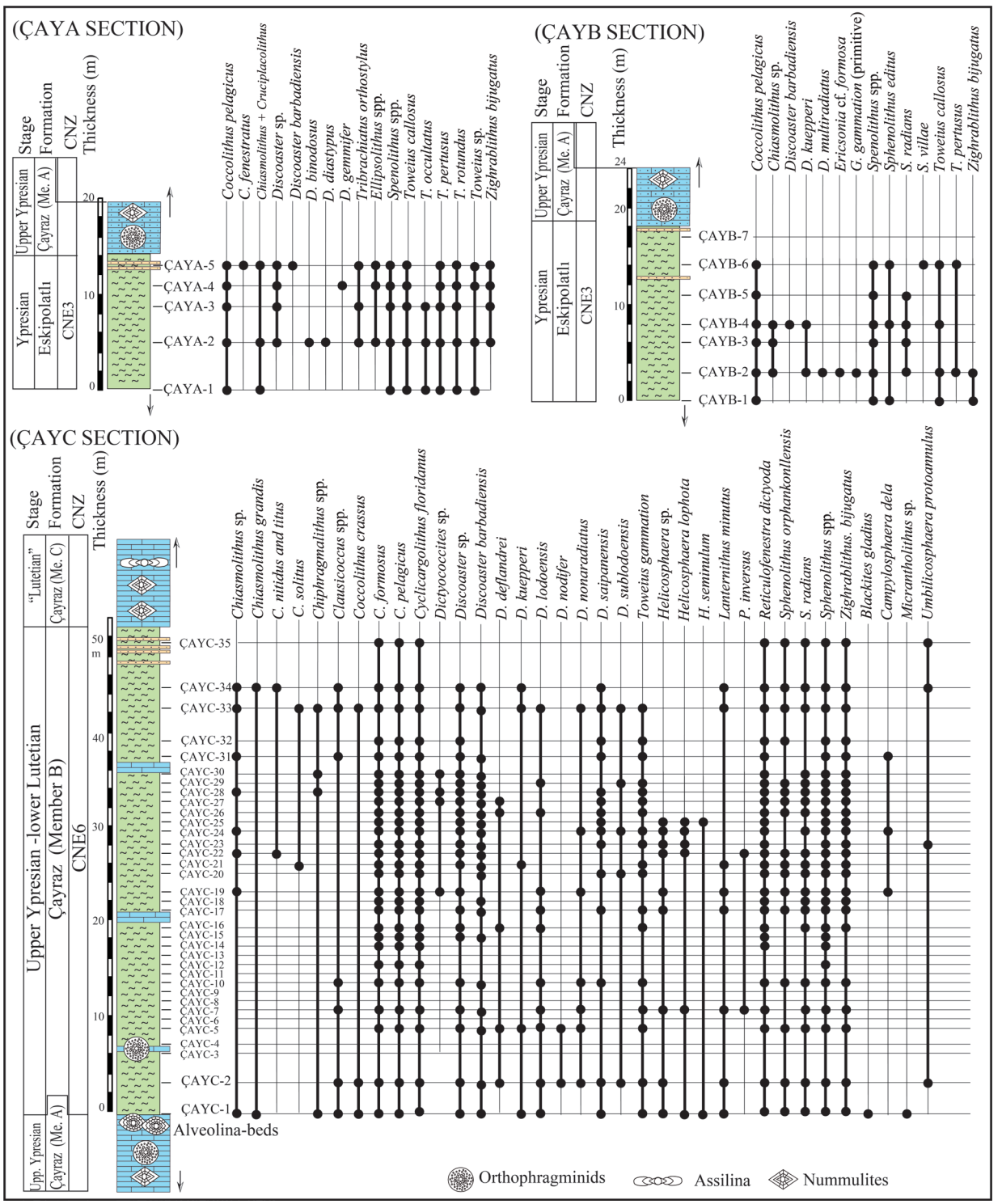

Figure 7. Distribution of calcareous nannofossils in sections ÇAYA and B (Eskipolatlı Fm.), and in section ÇAYC (Member B, Çayraz Fm.).

primitive form, *occultatus*, *pertusus*, *rotundus*) (Figures 8E–8G), *Ellipsolithus* (e.g., *macellus*) (Figure 8D), *Sphenolithus* (e.g., *moriformis* and *primus*) and *Zygrhablithus bijugatus* (Figure 8C). Consistent assemblages composed of *Discoaster diastypus* (Figure 8B), *Discoaster barbadiensis*, *D. kuepperi* (Figure 8K), *Sphenolithus editus* (Figure 8H), *Sphenolithus radians* (Figure 8I), *Sphenolithus villae* (Figure 8J), and *Tribrachiatus orthostylus* (Figure 8A) allow the dating of the section to the Ypresian CNE3p.p. Zone (corresponding to NP11 and CP9b zones).

Member B of the Çayraz Formation (Section ÇAYC) is also characterized by the dominant occurrence of reworked nannofossils, both Cretaceous and Paleocene in age (Figure 7). Nevertheless, in this section, the autochthonous nannofossils contain a higher number of species. Placolith group is the most represented, with a high number of forms referable to the species *Cyclicargolithus floridanus* (Figure 9B), *Reticulofenestra dictyoda* (Figure 9C), *Coccolithus formosus* (Figure 9E) and *C. pelagicus*, and a low number of forms referable to *Clausicoccus*, *Coccolithus crassus* (Figure 9A), *Chiasmolithus* and *Toweius gammation* (Figure 9D). Among the genus *Chiasmolithus*, it is possible to recognize *C. grandis*, *C. nitidus*, and *C. solitus*. The genus *Sphenolithus* is well represented and it is possible to distinguish the species *S. orphankonllensis* and *S. radians*, while all the specimens not recognizable at species level and specimens of *S. moriformis* are gathered under *Sphenolithus* spp. Among the genus *Helicosphaera*, it is possible to recognize *H. lophota* (Figure 9K) and *H. seminulum* (Figure 9L), which occur sporadically. The genus *Discoaster* is composed of frequent *D. barbadiensis* (Figure 9F), while the presence of the marker species *D. sublodoensis* (Figure 9J), *D. lodoensis* (Figure 9H), and *D. saipanensis* (Figure 9I) allows us to recognize the late Ypresian CNE6 Zone (corresponding to NP14p.p. and CP12ap.p. zones).

The upper part of the Member C of the Çayraz Formation is characterized by lithologies not very suitable for calcareous nannofossils (ÇAYD and ÇAYE sections, Figures 4 and 10). In particular, samples from ÇAYD section are barren or characterized by assemblages consisting of scarce specimens referable to a reduced number of taxa (*C. formosus*, *C. pelagicus*, *Discoaster* sp., and *R. dictyoda*) that do not allow a precise dating. Samples from the ÇAYE contain assemblages with a high number of specimens referable to the species *C. floridanus*, followed by the other placoliths *C. formosus*, *C. pelagicus* and *R. dictyoda*, and by the genus *Sphenolithus*; *D. barbadiensis*, *D. kuepperi*, and *H. seminulum* are very rare and occur only sporadically. These assemblages allow us to infer a wide interval of time that spans the late Ypresian-early Lutetian.

Lithologies more suitable for calcareous nannofossils occur in the sections ÇAYF, ÇAYG and ÇAYH, which correspond to Member D of the Çayraz Formation (Figures 4, 10-11). They contain assemblages with rare or no reworked forms. The autochthonous species are diverse and are represented by the specimens that present good to moderate preservation. Placoliths group shows high figures of *C. floridanus*, *R. dictyoda*, *C. formosus*, and *C. pelagicus*. The genus *Coccolithus* contains some biostratigraphically marker species such as *C. gigas* (Figure 12D), *C. mutatus* (Figure 12C), and *C. opdikey* (Figure 12A), while *Chiasmolithus* contains *C. grandis* (Figure 12B) and *C. solitus* (Figure 12 F). *Helicosphaera* is represented by *H. lophota* and *H. seminulum*. The genus *Sphenolithus* contains biostratigraphically index species, such as *S. furcatolithoides* (Figure 13G), *S. perpendicularis* (Figure 13J), and *S. spiniger* (Figure 13I). The genus *Discoaster* is mainly represented by the species *D. barbadiensis*, *D. deflandrei* (Figure 13D), *D. saipanensis*, *D. tanii* (Figure 13E), and by the significant species *D. bifax* (Figure 13F). Braarudosphaeraceae occur consistently and are mainly represented by *Braarudosphaera* and *Pemma* and *Michrantolithus* sp. *Braarudosphaera* occurs with *B. perampla* (Figure 13K) and *B. sequel* (Figure 13L) while *Pemma* is present with *P. papillatum* (Figure 12L). *Lanternithus minutus* (Figure 12I) and *Z. bijugatus* represent Holococcoliths. The occurrence of *Nannotetrina cristata* (Figure 13A) and *Nannotetrina alata* (Figure 13B) allows the identification of the Lutetian CNE9 Zone (corresponding to NP15 and CP13a zones) in the ÇAYF and ÇAYG section. In the ÇAYG section, the *C. gigas* from the sample of the ÇAYG4, suggests the transition to the CNE10 Zone (corresponding to CP13b), while the first occurrence of *S. furcatolithoides* better constrains the upper part of the section. The rare and discontinuous occurrence of *Reticulofenestra umbilicus* with *D. bifax* and *Nannotetrina*, allows us to recognize the CNE12 Zone (corresponding to NP15p.p.-NP16p.p. and CP13c zones) in the ÇAYH section.

4.2. Calcareous nannofossil paleoecology and paleoenvironment

The ecological preferences of Eocene calcareous nannofossils are not definitively known because the abundance of taxa can be affected by different factors such as temperature, salinity, nutrients, and turbidity, as well as the availability of sunlight. Moreover, species and genera can change behavior through time and among different biogeographical settings. However, there is general agreement that certain species reflect specific environmental conditions (e.g., Wei and Wise, 1990; Wei et al., 1992; Bralower, 2002; Gibbs et al., 2006; Villa et al., 2008), and below are reported the ecological preferences of key taxa used in this study.

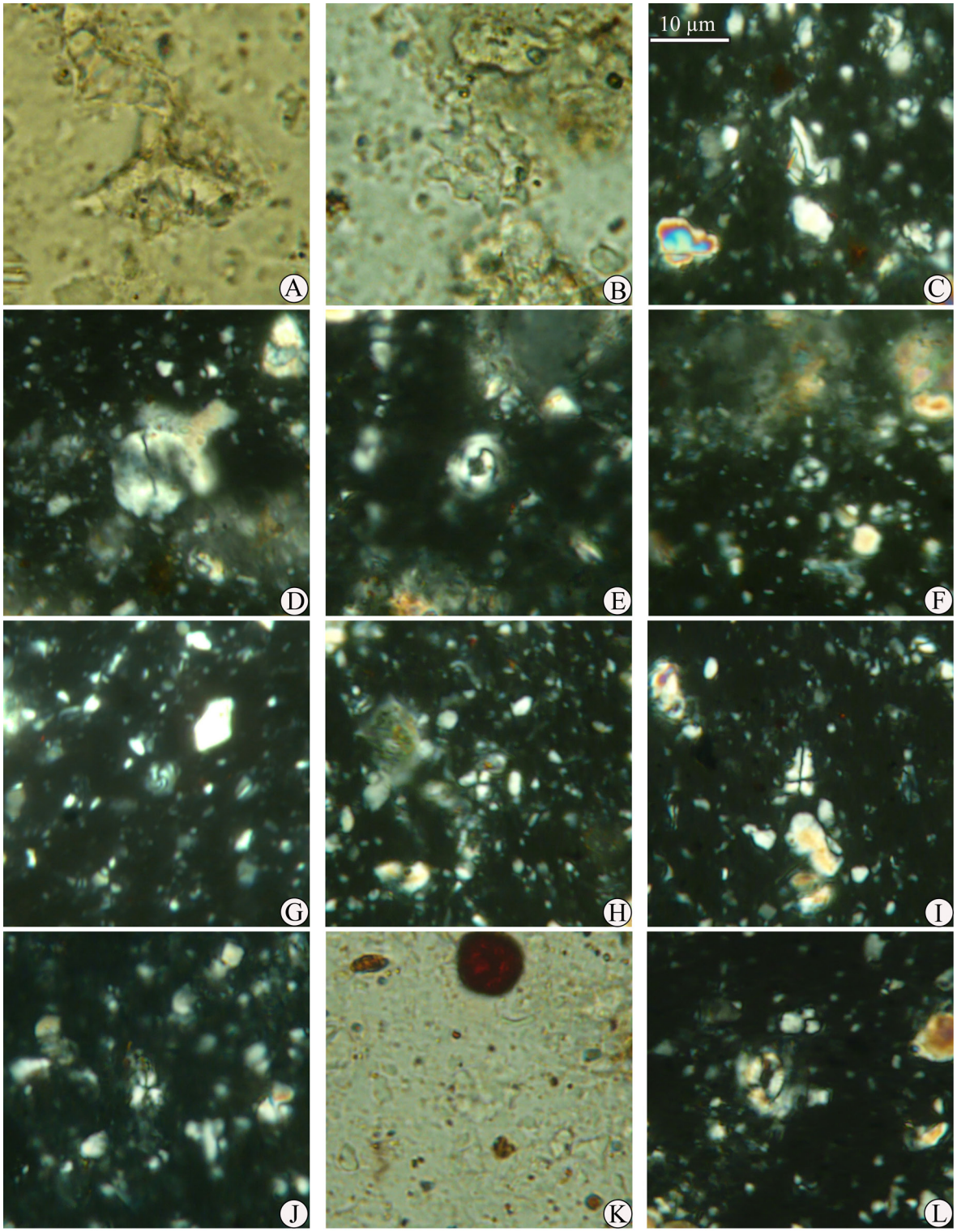

Figure 8. Microphotographs of selected calcareous nannofossil taxa from the upper part of the Eskipolatlı Formation. **A**) *Tribrachiatus orthostylus*, sample ÇAYA2. **B**) *Diascoaster diastypus*, sample ÇAYA2. **C**) *Zygrhablithus bijugatus*, sample ÇAYA2. **D**) *Ellipsolitus macellus*, sample ÇAYA2. **E**) *Toweius callosus*, sample ÇAYA4. **F**) *Toweius pertusus*, sample ÇAYA4. **G**) *Toweius gammation* (primitive specimen), sample ÇAYB2. **H**) *Sphenolithus editus*, sample ÇAYB4. **I**) *Sphenolithus radians*, sample ÇAYB4. **J**) *Sphenolithus villae*, sample ÇAYB6. **K**) *Discoaster kuepperi*, sample ÇAYB4. **L**) *Coccolithus pelagicus*, sample ÇAYB6.

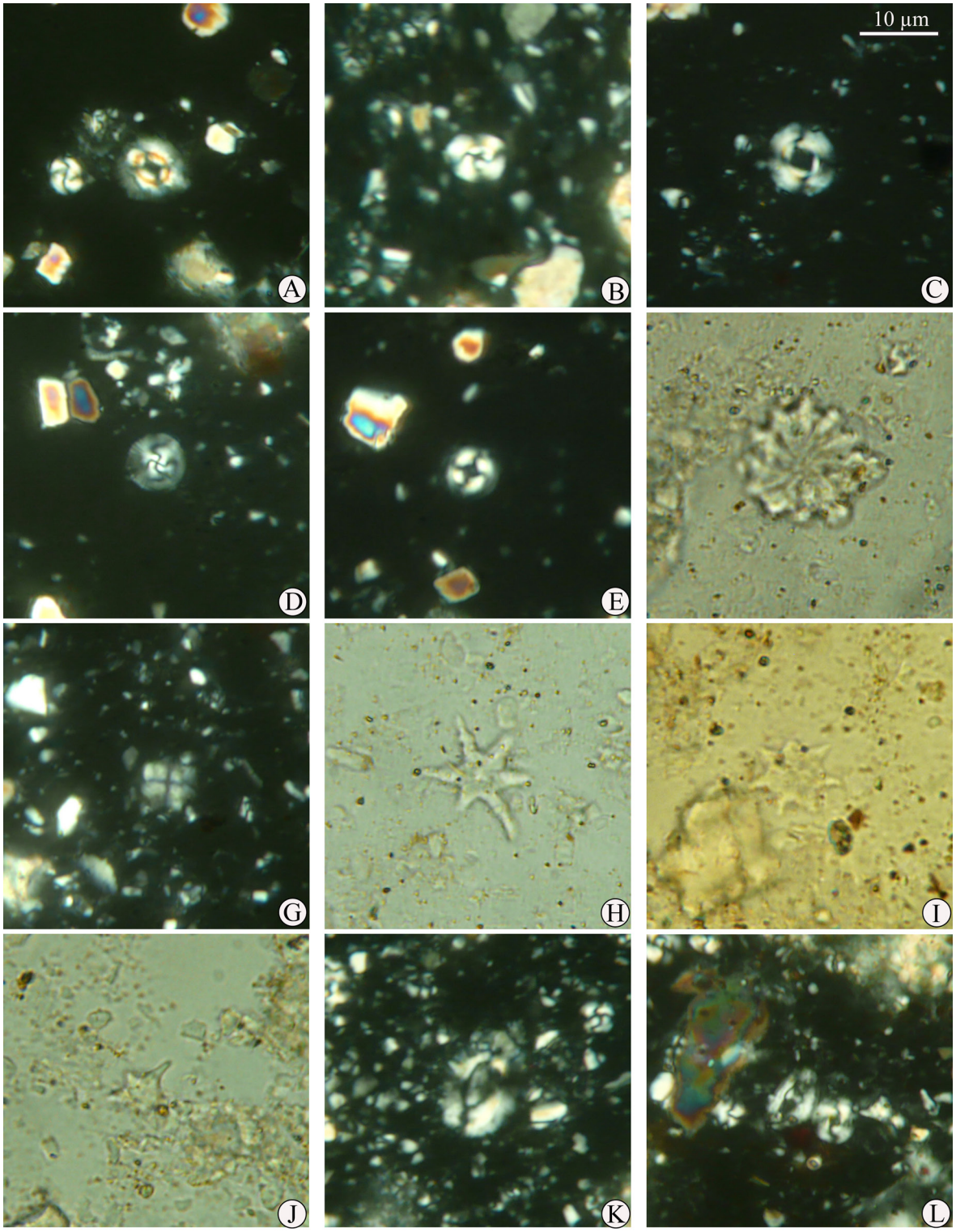

Figure 9. Microphotographs of selected calcareous nannofossil taxa from the Member B of the Çayraz Formation. **A**) *Coccolithus crassus*, sample ÇAYC2. **B**) *Cyclicargolithus floridanus*, sample ÇAYC2. **C**) *Reticulofenestra dictyoda*, sample ÇAYC2. **D**) *Toweius gammation*, sample ÇAYC2. **E**) *Coccolithus formosus*, sample ÇAYC2. **F**) *Discoaster barbadiensis*, sample ÇAYC2. **G**) *Discoaster kuepperi*, sample ÇAYC1. **H**) *Discoaster lodoensis*, sample ÇAYC2. **I**) *Discoaster saipanensis*, sample ÇAYC32. **J**) *Discoaster sublodoensis*, sample ÇAYC2. **K**) *Helicosphaera lophota*, sample ÇAYC1. **L**) *Helicosphaera seminulum*, sample ÇAYC1.

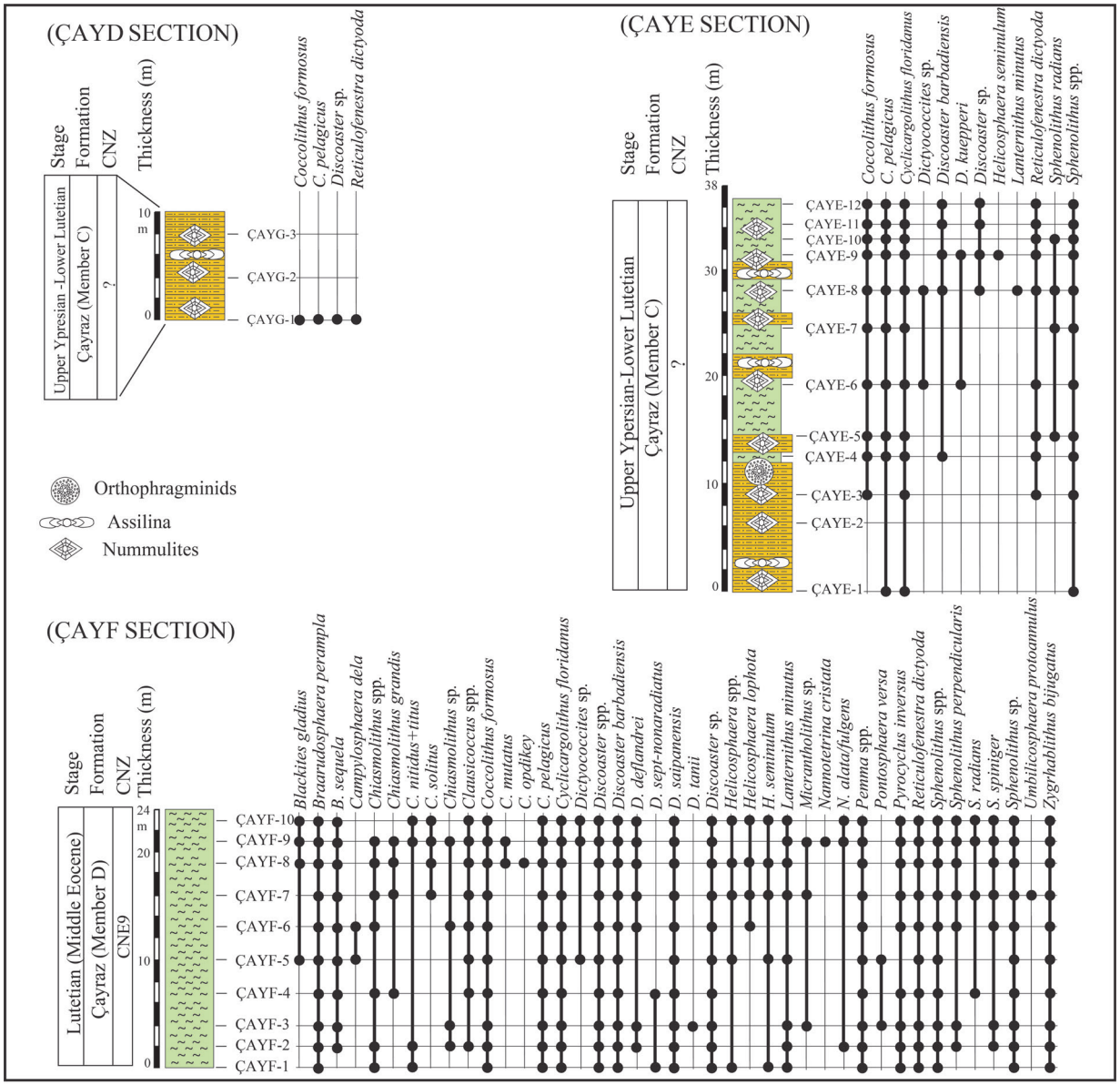

Figure 10. Distribution of calcareous nannofossils in the upper part of the Member C (sections ÇAYD and ÇAYE) and Member D of the Çayraz Formation (section ÇAYF).

Coccolithus pelagicus is regarded as eumesotrophic warm water species (Haq and Lohman, 1976; Bukry, 1981; Wei and Wise, 1990). The genus *Toweius* is considered to have a preference for mesoeutrophic water (Bown et al., 2004), but some authors suggested that the species *T. occultatus* and *T. callosus* were adapted to warm, mesotrophic conditions (Self-Trail et al., 2012). The genus *Discoaster* is commonly recognized as a warm and oligotrophic taxa (Edwards, 1968; Bukry, 1973; Wei and Wise, 1990; Gibbs et al., 2006; Angori et al., 2007; Villa et al., 2008; Schneider et al., 2011). The genus *Sphenolithus* seems better adapted to oligotrophic and warm-water conditions (Aubry, 1998; Bralower, 2002; Gibbs et al., 2006; Agnini et al., 2007; Schneider et al., 2011; Kalb and Bralower 2012). *Cyclicargolithus foridanus* has been associated with high-productivity environments (Aubry, 1992; Monechi et al., 2000; Dunkley Jones et al., 2008) and warm to temperate water (Wei and Wise, 1990). *Reticulofenestra dictyoda* had affinity to mesoeutrophic temperate water as suggested by Wei and Wise (1990), Villa et al. (2008), Schneider et al. (2011). *Coccolithus formosus* had a preference for warm and oligotrophic water (Monechi et al., 2000; Bralower, 2002; Gibbs et al., 2006; Angori et al., 2007; Villa et al., 2008; Schneider et al., 2011). The genus *Chiasmolithus*

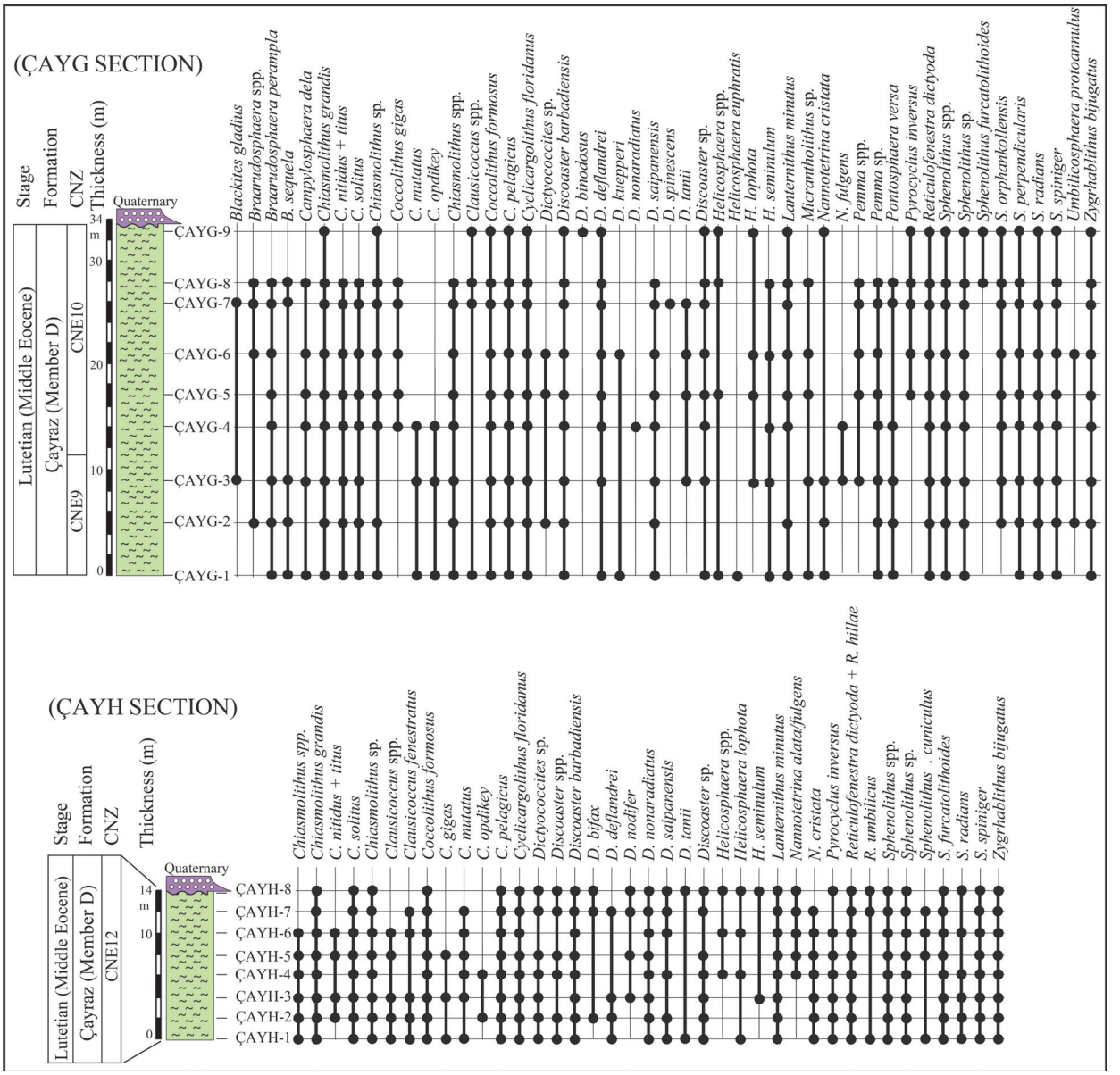

Figure 11. Distribution of calcareous nannofossils in sections ÇAYG and ÇAYH, Member D of the Çayraz Formation.

is largely regarded as preferring cool eutrophic water conditions (Wei and Wise, 1990; Aubry, 1992; Bralower, 2002; Persico and Villa, 2004; Tremolada and Bralower, 2004; Villa et al., 2008).

Lanternithus minutus and *Z. bijugatus* have been considered adapted to warm/temperate and oligotrophic water (Kleijne, 1991; Aubry, 1998; Bralower, 2002; Agnini et al., 2006; Gibbs et al., 2006).

Braarudosphaeraceae are mostly associated with shallow epicontinental seas (Bybell and Gartner, 1972; Perch-Nielsen, 1985; Siesser et al., 1992) so indicating eutrophic water with high turbidity and low salinity (Bramlette and Martini, 1964; Müller, 1976; Bukry, 1973; Armstrong and Brasier, 2005). The genus *Helicosphaera* had an affinity to warm eutrophic water (Perch-Nielsen, 1985; Wei and Wise, 1990; Giorgioni et al., 2019).

Based on abundances of calcareous nannofossil, it is possible to infer paleoclimatic and paleoenvironmental conditions in the Haymana Basin during the early-middle Eocene. The assemblages recognized in the Eskipolatli Formation suggest a deposition environment characterized by warm eumesotrophic water. In fact, *Toweius* and *C. pelagicus* occur with high percentages (up to 40% and up to 36%, respectively, in ÇAYA section), while the common occurrence of sphenoliths (up to 22% in ÇAYA section) supports warm water conditions. The decline in calcareous

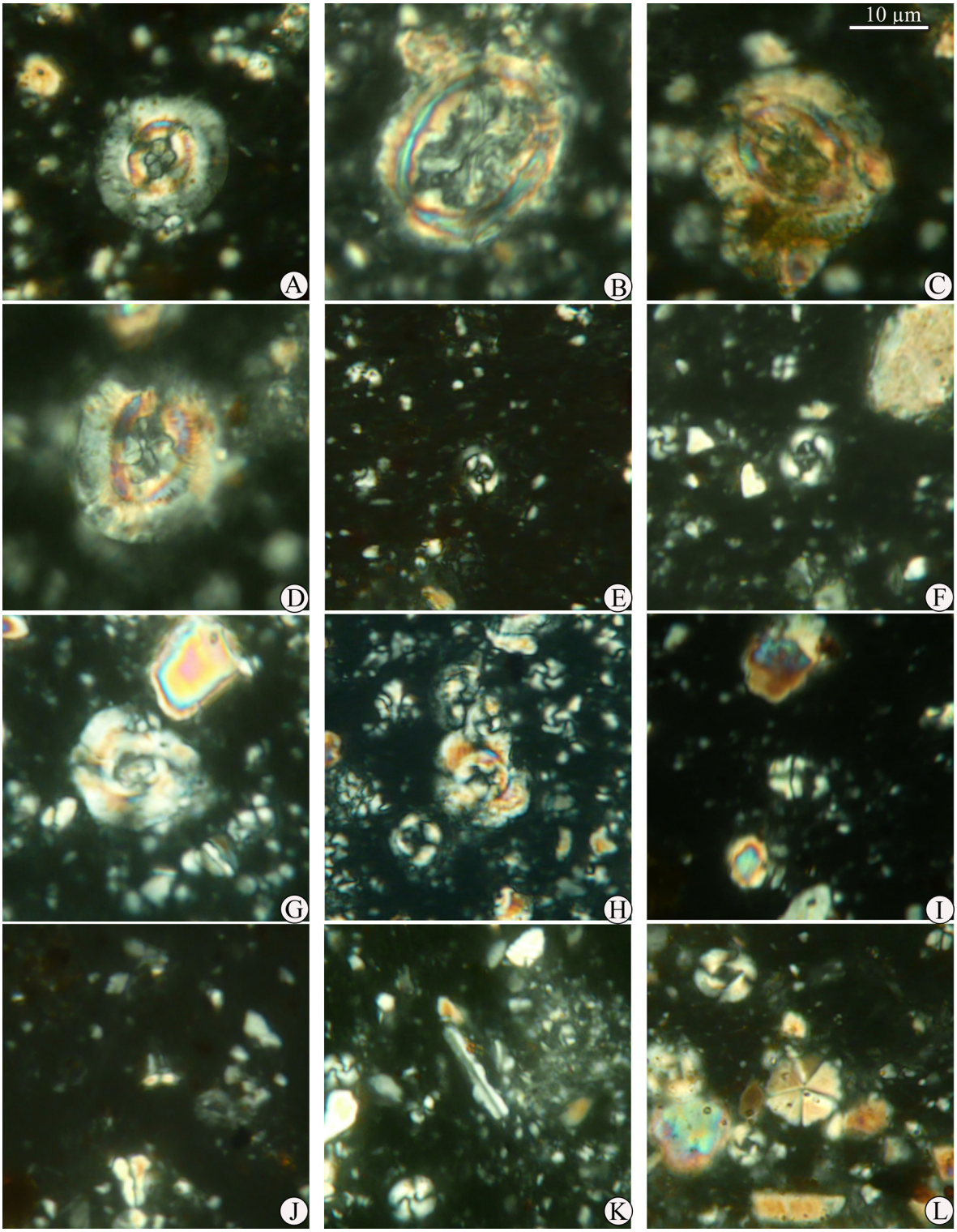

Figure 12. Microphotographs of selected calcareous nannofossil taxa from the Member D of the Çayraz Formation. **A)** *Coccolithus opdikey*, sample ÇAYG4. **B)** *Chiasmolithus grandis*, sample ÇAYG9. **C)** *Coccolithus mutatus*, sample ÇAYG4. **D)** *Coccolithus gigas*, sample ÇAYG4. **E)** *Chiasmolithus nitidus*, sample ÇAYG4. **F)** *Chiasmolithus solitus*, sample ÇAYG4. **G)** *Reticulofenestra umbilicus*, sample ÇAYH7. **H)** *Reticulofenestra hillae*, sample ÇAYH7. **I)** *Lanternithus minutus*, sample ÇAYH6. **J)** *Blackites gladius*, sample ÇAYG7. **K)** *Pseudotriquetrorhabdulus inversus*, sample ÇAYG8. **L)** *Pemma papillatum*, sample ÇAYG7.

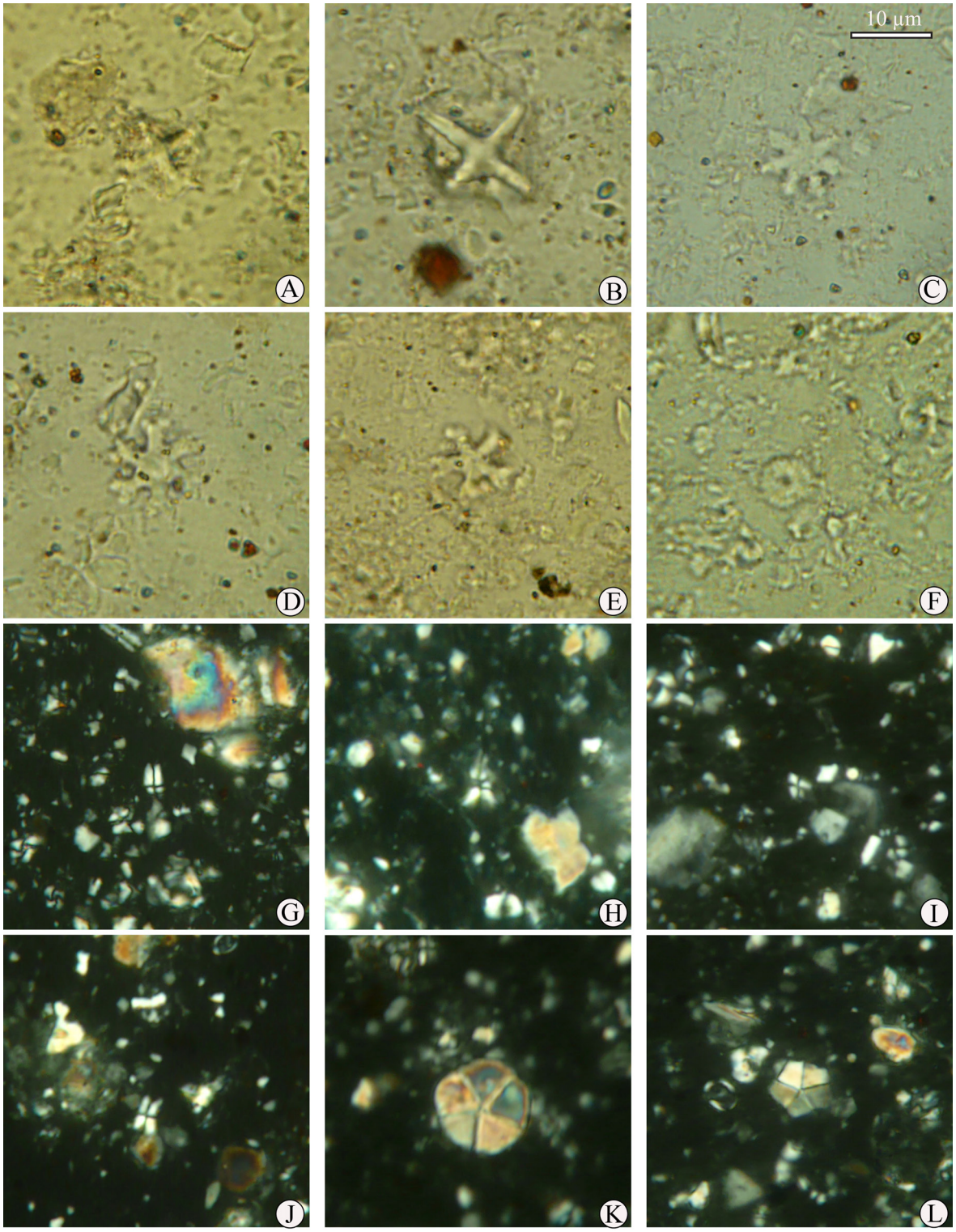

Figure 13. Microphotographs of selected calcareous nannofossil taxa from Member D of the Çayraz Formation. **A)** *Nannotetrina cristata*, sample ÇAYG3. **B)** *Nannotetrina alata*, sample ÇAYG3. **C)** *Discoaster binodosus*, sample ÇAYG9. **D)** *Discoaster deflandrei*, sample ÇAYG3. **E)** *Discoaster tanii*, sample ÇAYG3. **F)** *Discoaster bifax*, sample ÇAYH7. **G)** *Sphenolithus furcatolithoides*, sample ÇAYG9. **H)** *Sphenolithus orphanknollensis*, *sample* ÇAYG9. **I)** *Sphenolithus spiniger*, sample ÇAYG9. **J)** *Sphenolithus perpendicularis*, sample ÇAYG1. **K)** *Braarudosphaera perampla*, sample ÇAYG2. **L)** *Braarudosphaera sequela*, sample ÇAYG2.

nannofossils in the ÇAYB section suggests shallower water depths and sediments from a more proximal, coastal setting within the basin compared to the ÇAYA section. The Member B of the Çayraz formation (ÇAYC section) contains assemblages primarily characterized by eutrophic and warm water taxa (*C. floridanus*, *C. pelagicus*, *C. formosus*, *R. dictyoda*). The common occurrence of sphenoliths (up to 25%) and discoasterids confirm warm water conditions. In the overlying Member C, nannoplanktons suffered low diversity (ÇAYD and ÇAYE sections), assemblages contain a high abundance of taxa supporting eutrophic conditions (*C. floridanus*) while taxa adapted to warm, oligotrophic, and mesotrophic water (*Discoaster*, *Sphenolithus*, *C. pelagicus*, *R. dictyoda*, *Z. bijugatus*) disappear or show fluctuation. In general, lower diversity assemblages with abundant meso-/eutrophic taxa occur in highly eutrophic environments with high concentrations of nutrients. This suggests that the basin turned into a more productive environment associated with enhanced terrigenous supply from the land. In addition, reduction in warm water taxa can be linked to the global post-Early Eocene Climatic Optimum (EECO) cooling phase (Westerhold et al., 2018) that coincides with the late Ypresian-early Lutetian time span detected in Member C.

Assemblages from the Member D are highly diversified. High percentages of *C. floridanus* (up to 74% in ÇAYG) indicate eutrophic water and the common occurrence of *R. dictyoda* indicate warm-temperate water. The occurrence of cool-water taxa (*Chiasmolithus*) and warm-water taxa (*Discoaster*, *Sphenolithus*) led us to think about temperate conditions to which both taxa were able to adapt. The constant nutrient availability is also confirmed by the presence of braarudosphaerids (e.g., *B. perampla*, *B. sequela*, *Pemma* spp., in ÇAYF and ÇAYG sections).

4.3. Planktonic foraminifera biostratigraphy

Planktonic foraminiferal assemblages are moderately abundant, diverse, and generally well-preserved throughout the section ÇAYF. They are dominated by *Acarinina*, with less common occurrences of *Subbotina* and *Parasubbotina* (Figure 14). *Acarinina* is represented by *A. bullbrooki*, *A. boudreauxi* (Figure 15. 5a-c) and *A. pseudosubsphaerica* (Figure 15. 1a-b), *Subbotina* by *S. linaperta* and *S. roesnaesensis* (Figure 15. 12a-b) and *Parasubbotina* by *Parasubbotina inaequispira*. *Guembelitrioides nuttalli*, an invaluable marker of the Lutetian, and *Turborotalia frontosa* are minor components of the assemblages whereas *Pearsonites* (*P. anapetes*) and *Morozovelloides* (*M. bandyi* and *M. crassatus*) are recorded in only sporadic occurrences (Figure 15. 15a-c, 16a-b). In the lack of *Globigerinatheka kugleri*, these assemblages allow for ascribing the ÇAYF section to the E8 Zone (Berggren and Pearson, 2005; Wade et al., 2011). Small benthic foraminifera are represented by a limited number of specimens, including *Lenticulina*, *Bulimina*, *Melonis* along with rotaliid, miliolid, and nodosariid forms whereas ostracod and gastropod are found in only a few specimens in the assemblages from the ÇAYF section.

All samples from the ÇAYH section contain very rich, moderately diversified, and preserved planktonic foraminiferal assemblages with the dominance of *Subbotina* and *Acarinina*. *Subbotina* is represented by *S. eocaena* (Figure 15. 9a-b) and *S. senni* (Figure 15. 13a-b). *Acarinina* is represented by *A. bullbrooki* (Figure 15. 4a-c), *A. boudreauxi* and *A. praetopilensis* (Figure 15. 6a-b). *Hantkenina* (*H. liebusi*- Figure 16. 16a-c), *Globigerinatheka* (*G. kugleri* -Figure 16. 4a-c and *G. subconglobata*- Figure 16. 5a-b) and *Pearsonites* (*P. broedermanni*- Figure 15. 11a-b and *P. anapetes*- Figure 15. 8a-b) are distinctive and consistently occurring components of the assemblages. *G. nuttalli* frequently occurs with typical specimens having a relatively large, high-spired and loosely coiled tests with supplementary apertures in all samples (Figure 16. 1a-b). These assemblages allow the recognition of the E9-E10 zonal interval based on the concurrent ranges of *G. nuttalli* and *G. kugleri*. Although the absence of *Morozovella aragonensis* makes differentiation of the two zones difficult, common occurrences of *P. broedermanni* and *P. anapetes* provide reliable biostratigraphic evidence for determining the E9 Zone because they have stratigraphic ranges ending at the top of this zone. This zonal assignment is further supported by the common *A. boudreauxi* and rare *A. cuneicamerata* because their last occurrences are also documented in the E9 Zone (Berggren et al., 2006). *Pseudohastigerina micra* (Figure 16. 11a-b) occurs more frequently in both fine and coarse fractions of the ÇAYF samples than those in the ÇAYH section, where it is usually restricted to the fine fraction (between 63 and 125 μm) but is almost absent in the coarse fraction (>125 μm). *Paragloborotalia griffinoides* (Figure 16. 15a-b), *Planorotalites capdevilensis*, and *Globorotalides suteri* (Figure 16. 14a-b) are always minor components of the assemblages from both sections.

Although a quantitative analysis was not performed, planktonic foraminifera is the main component in all samples from the ÇAYH section and seems to represent almost >90% of the total foraminiferal content, thus suggesting a deep, open marine environment. Considering the composition of the planktonic foraminiferal assemblage a high proportion of deep-dwelling *Subbotina*, *Turborotalia*, *Hantkenina*, and *G. nuttalli* clearly indicates deep, relatively stable environment (Boersma et al., 1987; Pearson et al., 1993, 2001; Luciani et al., 2010).

5. Discussion

5.1. Revised stratigraphy of the Çayraz Formation by new paleontological and lithostratigraphic data

The Çayraz Formation is subdivided into four members based on their characteristic lithological features and the fauna identified in this study.

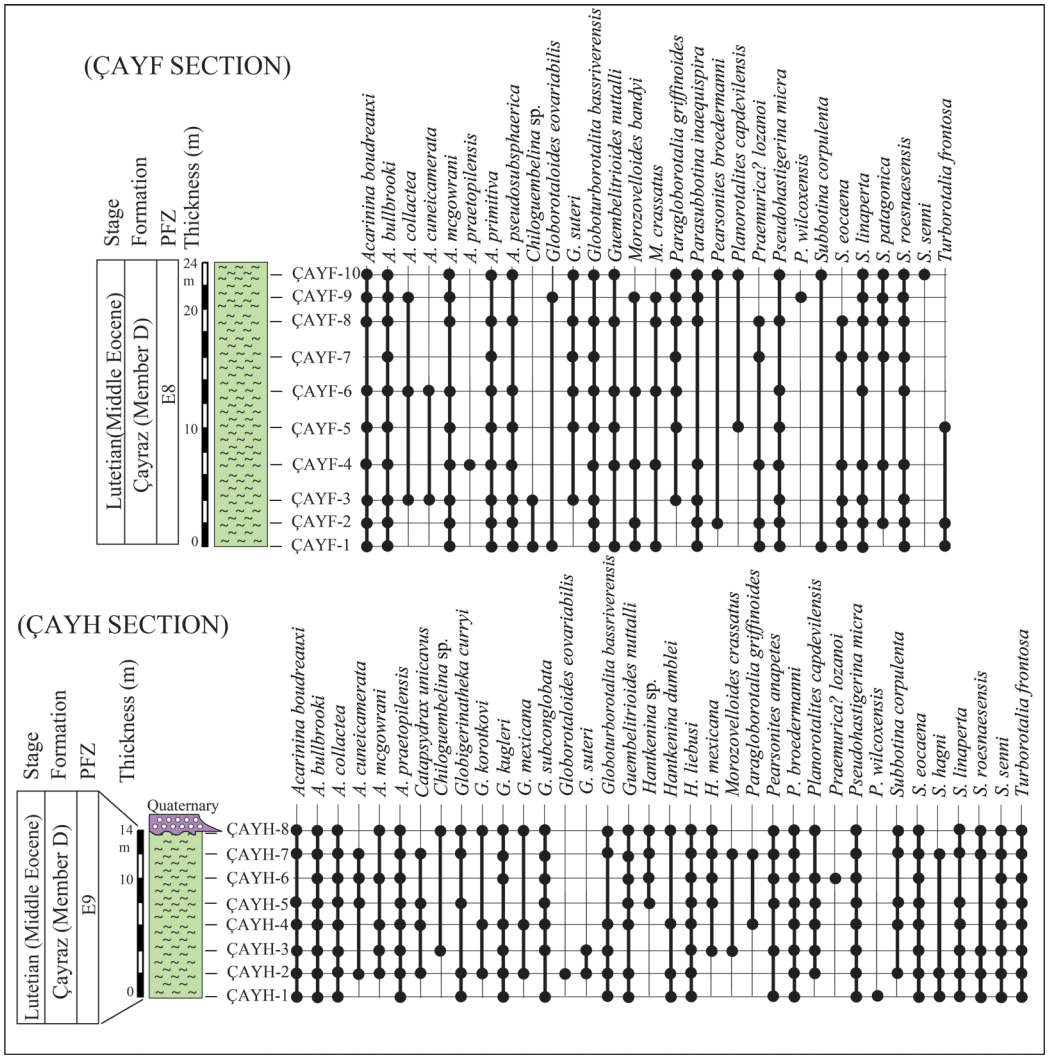

Figure 14. Distribution of planktonic foraminifera in sections ÇAYF and ÇAYH (Member D of the Çayraz Formation).

5.1.1. Member A

It represents a mixed carbonate-siliciclastic sequence (approximately 100/110-m-thick) characterized by the abundant occurrence of LBF and subordinate gastropoda, echinodermata, red algae, and very sporadic solitary corals and bivalves. The lower 25 m of the unit consists predominantly of sandy limestone beds intercalated with marly/silty alternation containing orthophragminids and nummulitids, which are assigned to shallow benthic zones (SBZ) 9/10 (early-late Ypresian transition) (Özcan et al., 2020). Relatively abundant *Discocyclina* Gümbel, *Orbitoclypeus* Silvestri, and *Asterocyclina* Gümbel and sporadic planktonic foraminifera at the lower part suggest open marine depositional conditions such as middle to outer-ramp settings. The orthophragminids belong to *Discocyclina augustae* van der Weijden, *D. 'dispansa'* (Sowerby), *D. trabayensis* Neumann, *D. archiaci* (Schlumberger), *D. fortisi* (d'Archiac), *Nemkovella evae* Less, *N. strophiolata* (Gümbel), *O. schopeni* (Checchia-Rispoli), *O. douvillei* (Schlumberger) and *O. munieri* (Schlumberger) (Özcan, 2002). Several lenticular micritic limestone beds may suggest the formation of mud-mounds with rare corals and bivalves. This is followed by a monotonous sequence of thick-bedded calcarenites consisting of mainly nummulitids (*Assilina* d'Orbigny and *Nummulites* Lamarck along with rare *Operculina* d'Orbigny) and rare *Discocyclina* and *Orbitoclypeus*. Towards the upper part of Member A, an alternation of marly/silty beds with LBF and nummulitic accumulations consisting of *Nummulites*, *Assilina*, and rare *Discocyclina* and *Orbitoclypeus* (*D. archiaci*, *D. fortisi*, *O. douvillei*) are observed. A distinct interval of thin-bedded limestone

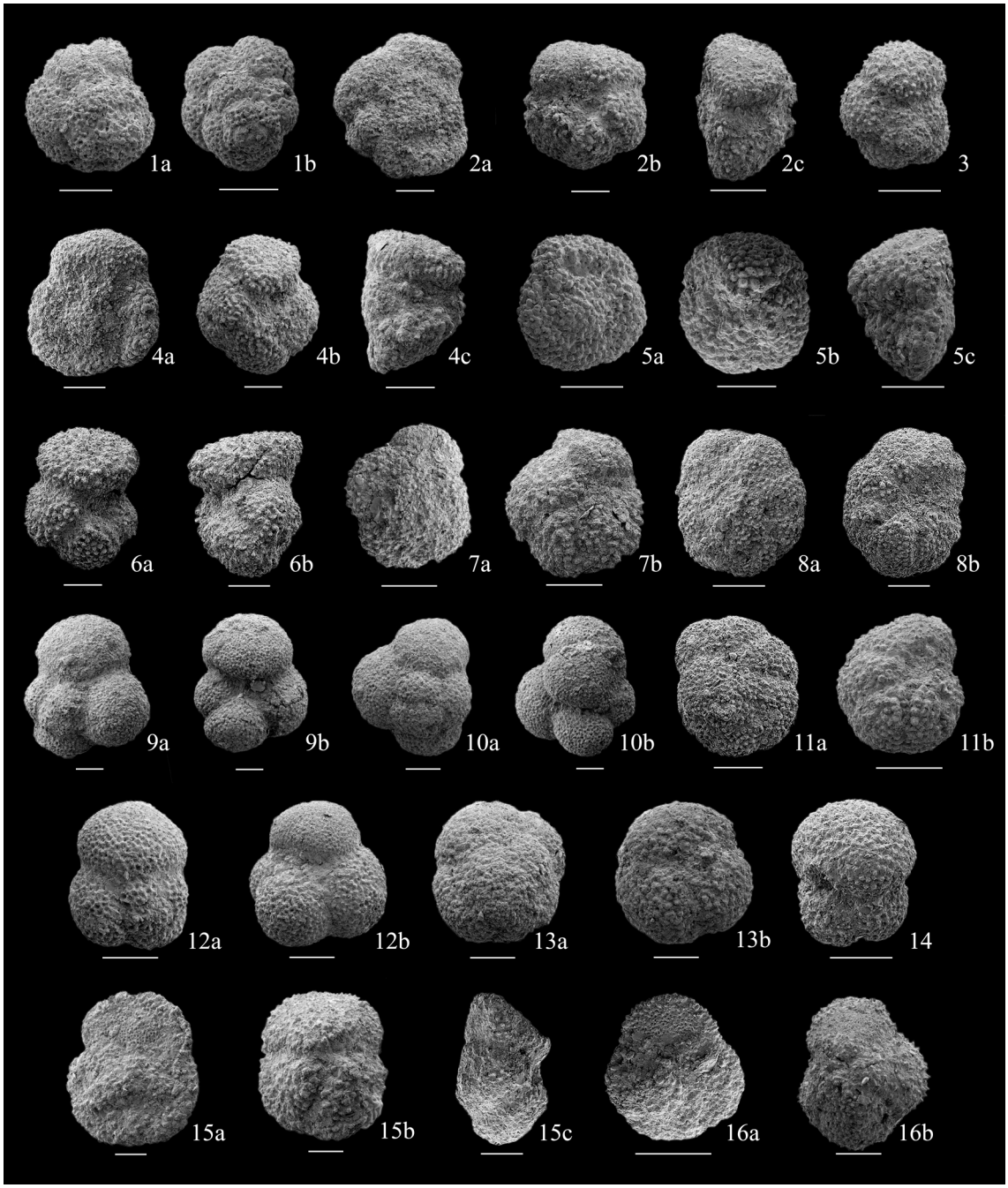

Figure 15. SEM photographs of selected planktonic foraminifera from the Member D of the Çayraz Formation. **1a, b)** *Acarinina pseudosubsphaerica*, a, b- spiral view, samples ÇAYF1, ÇAYF2; **2a-c)** *Acarinina cuneicamerata*, a- spiral view, b- umbilical view, c- side view, samples ÇAYH7, ÇAYH2; **3)** *Acarinina mcgowrani*, spiral view, sample ÇAYH3; **4a-c)** *Acarinina bullbrooki*, a- spiral view, b- umbilical view, c- side view, sample ÇAYH7; **5a-c)** *Acarinina boudreauxi*, a- spiral view, b- umbilical view, c- side view, sample ÇAYF4; **6a, b)** *Acarinina praetopilensis*, a- umbilical view, b- umbilical view, sample ÇAYH8; **7a, b)** *Acarinina collactea*, a- spiral view, b- umbilical view, sample ÇAYH2; **8a, b)** *Pearsonites anapetes*, a- spiral view, b- umbilical view, sample ÇAYH5; **9a, b)** *Subbotina eocaena*, a- spiral view, b- umbilical view, sample ÇAYH8; **10a, b)** *Subbotina corpulenta*, a- spiral view, b- umbilical view, sample ÇAYH4; **11a, b)** *Pearsonites broedermanni*, a- spiral view, b- umbilical view, sample ÇAYH4; **12a, b)** *Subbotina roesnaesensis*, a- spiral view, b- umbilical view, sample ÇAYF3; **13a, b)** *Subbotina senni*, a- spiral view, b- umbilical view, sample ÇAYH3; **14)** *Subbotina linaperta*, umbilical view, sample ÇAYH9; **15a-c)** *Morozovelloides bandyi*, a- spiral view, b- umbilical view, c- side view, samples ÇAYF1, ÇAYF6; **16a, b)** *Morozovelloides crassatus*, a- spiral view, b- umbilical view, samples ÇAYF1, ÇAYF4. Scale bar: 100 μm.

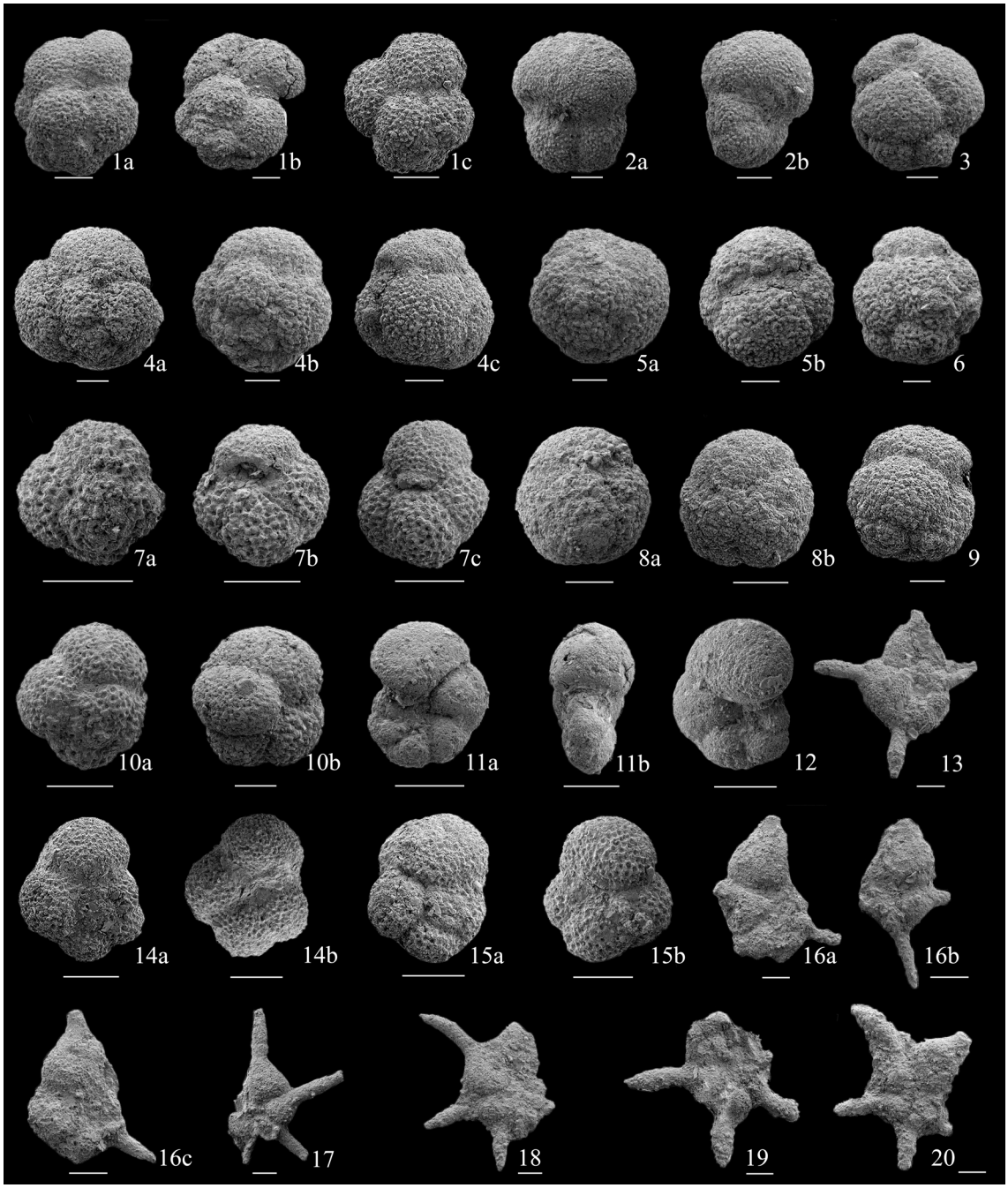

Figure 16. SEM photographs of selected planktonic foraminifera from Member D of the Çayraz formation. **1a-c)** *Guembelitrioides nuttalli*, a-c- spiral view, samples ÇAYH4, ÇAYH7, ÇAYF2; **2a,b)** *Turborotalia frontosa*, a- umbilical view, b- side view, sample ÇAYH6; **3)** *Globigerinatheka korotkovi*, side view, sample ÇAYH2; **4a-c)** *Globigerinatheka kugleri*, a- spiral view, b- oblique view, c- side view, samples ÇAYH8, ÇAYH6; **5a,b)** *Globigerinatheka subconglobata*, a- spiral view, b- umbilical view, sample ÇAYH4; **6, 9)** *Globigerinatheka curryi*, 6- spiral view, 9- side view, sample ÇAYH1; **7a-c)** *Globoturborotalita bassriverensis*, a- spiral view, b- c- umbilical views, samples ÇAYF1, ÇAYF2; **8a, b)** *Globigerinatheka mexicana*, a- umbilical view, b- spiral view, sample ÇAYH8; **10a, b)** *Catapsydrax unicavus*, , a- spiral view, b- c- umbilical view, sample ÇAYH2; **11a, b)** *Pseudohastigerina micra*, a- peripheral view, b- side view, sample ÇAYF2; **12)** *Pseudohastigerina wilcoxensis*, peripheral view, sample ÇAYF9; **13)** *Hantkenina* sp., sample ÇAYH6; **14a, b)** *Globorotaloides suteri*, a- spiral view, b- c- umbilical view, sample ÇAYF3; **15a, b)** *Paragloborotalia griffinoides*, a- spiral view, b- c- umbilical view, sample ÇAYF9; **16a-c)** *Hantkenina liebusi*, samples ÇAYH7, ÇAYH2, ÇAYH8; **17)** *Hantkenina mexicana*, sample ÇAYH8; **18)** *Hantkenina* sp., sample ÇAYH6; **19)** *Hantkenina* sp., sample ÇAYH7; **20)** *Hantkenina* sp., sample ÇAYH5. Scale bar: 100 μm.

beds composed of mudstone with dasycladalean algae, and bivalve shells have been recorded in the upper part (Özcan et al., 2020). A significant change in the depositional setting is marked by *Alveolina*-limestone level at the uppermost part of Member A. The *Alveolina*-beds are outlined by a nodular to conglomeratic horizon of micritic limestone pebbles with alveolinids and nummulitids. The nodules (5–15 cm in diameter) are rounded and often elongated and contain iron stains, especially at their contacts. Heavy burrowing observed within the calcareous matrix between the nodules indicates reworking and redeposition in a shallow marine setting prior to the drowning of the platform. Orthophragminids and alveolinids in the upper part of Member A suggest SBZ 12, indicating the latest Ypresian age (Özcan et al., 2020). Hottinger (1960) reported some *Alveolina* assemblages from Member A, but it is impossible to discern their exact position. The author reported the presence of *Alveolina canavarii* Checcia-Rispoli, *A.* cf. *schwageri* Checcia-Rispoli, *A. pinguis* Hottinger and erected a new species, *A. lehneri* from the 'middle Cuisian' beds. Type-level of the species ('Coupe 5, Couche 1' in Hottinger, 1960) is most probably located at the upper part of Member A, though exact stratigraphic position of this species remains dubious. *Alveolina lehneri* appears to be key for SBZ11 ('middle late Ypresian), partly extending into SBZ12 in Serra-Kiel et al. (1998). The stratigraphic position of *Alveolina çayrasi* Dizer (1964), originally established from the supposedly lower Lutetian beds (herein Member C) of the Çayraz Formation (Dizer, 1964, 1968) is not also certain. This species is marked as a biostratigraphically significant species for SBZ13 (early Lutetian) by Serra-Kiel et al. (1998). However, this was challenged by Sirel and Acar (2008) proposing that *A. çayrasi* (*A. çayrazensis* in Sirel and Acar, 2008) is, in fact, a marker for 'middle Cuisian' (middle late Ypresian). Sirel and Deveciler (2017) reported this species from the levels that correspond to Member A. Schaub (1981) described the occurrence of *Nummulites burdigalensis* de la Harpe, *N. leupoldi* Schaub, *N. partschi* de la Harpe, *N. irregularis* Deshayes, *N. kaufmanni* Mayer and *Assilina placentula* (Deshayes) from levels corresponding to samples 113-119 of Hottinger (1960) from Member A. All these taxa are characteristic for the late Ypresian (SBZ10-12 in Serra-Kiel et al., 1998). Sirel and Deveciler (2017) reported *Nummulites planulatus* (Lamarck) and *N. irregularis* in the lower part of Member A and *N. partschi*, *N. burdigalensis*, *Assilina placentula*, *Coskinolina liburnica* Stache, *Cuvillierina vallensis* (Ruiz de Gaona), *Lockhartia conditi* (Nuttall), *Alveolina canavari*, *A. bayburtensis* Sirel, *A. cremae* Checcia-Rispoli, *A. çayrazensis* Dizer, *A. oblonga* d'Orbigny, *A. schwageri*, *A.* aff. *cuspidate* Drobne, *A.* cf. *boscii* (Defrance in Broon), *Glomoalveolina minutula* Reichell in Renz, *Granorotalia sublobata* Benedetti, Di Carlo and Pignatti, *Ornatorotalia spinosa* Benedetti, Di Carlo and Pignatti and *Asterigerina çayrazensis* Sirel and Deveciler in the 'middle' and upper parts of the same member and assigned a late Ypresian age. Moreover, the phylogenetic histories of two Tethyan orthophragminid lineages (*O. fortisi* (d'Archiac) and *O. douvillei* (Schlumberger)) were partly established from the Member A. *Discocyclina fortisi* consists of four successive chronospecies as *D. fortisi fortisi* (d'Archiac), *D. fortisi simferopolensis* Less, *D. fortisi anatolica* Özcan and Less and *D. fortisi cairazensis* Özcan, the last two of which were originally established from the Member A. *D. fortisi anatolica* is representative for orthophragminid Zone (OZ) 8a (SBZ 11; Ypresian) and *D. fortisi cairazensis* for OZ8b-9 (SBZ12-13/14?; late Ypresian- early Lutetian (Özcan, 2002; Özcan et al., 2007). *Asterigerina çayrazensis* was originally established from the Member A (Sirel and Deveciler, 2017). Member A contains more clastic material westward in the Çayraz region and suggests a very shallow marine to continental conditions with poor fauna (Özcan et al., 2020).

5.1.2. Member B

It represents a marly-silty sequence (approximately 50-m-thick and notably variable in thickness along an E-W transect) with calciturbiditic beds containing resedimented LBFs, common at its lower part. The most primitive member of *Discocyclina spliti* lineage, *D. spliti polatlıensis* Özcan and Less, and a new subspecies of *Orbitoclypeus varians* lineage, *O. varians ankaraensis* Özcan and Less were established initially from this unit (Özcan et al., 2007, 2022). Özcan et al. (2007) reported an assemblage of orthophragmines belonging to *Discocyclina augustae*, *D. dispansa*, *D. fortisi cairazensis* Özcan (the most advanced developmental stage of *D. fortisi* lineage), *D. senegalensis* Abrard, *Nemkovella evae karıtensis* Özcan and Less, and *Asterocyclina schweighauseri* Less. The nummulitids occur abundantly but are unidentified at species level in the previous studies. The calcareous nannofossils are characterized by the dominant occurrence of reworked Cretaceous and Paleocene forms. The autochthonous species such as *Cyclicargolithus*, *Reticulofenestra*, *Coccolithus, Clausicoccus*, *Chiasmolithus, Girgisia, Sphenolithus*, *Helicosphaera*, and *Discoaster. Discoaster* is frequently composed of *D. barbadiensis*, *D. sublodoensis*, *D. lodoensis*, and *D. saipanensis* indicating late Ypresian CNE6 Zone (corresponding to NP14p.p. and CP12ap.p. zones), along with the occurrence of *Coccolithus crassus*.

Planktonic foraminifera from the Member B are characterized by a dominant occurrence of *Acarinina* including *A. cuneicamerata*, *A. pentacamerata*, *A. bullbrooki*, *A. collactea*, *A. praetopilensis*. *Acarinina soldadoensis*, *A. angulosa*, and subordinate *A.*

pseudosubsphaerica (Özcan et al., 2020). They are associated with scarce *Pearsonites broedermanni*, *Subbotina senni*, *Parasubbotina inaequispira*, *S. eocaena*, *Morozovella crater*, *M. aragonensis*, and *M. caucasica*. This planktonic foraminiferal assemblage suggests P9 Zone (E7 Zone) of the latest Ypresian-early Lutetian transition (Wade et al., 2011).

5.1.3. Member C

This unit (approximately 155-m-thick) is characterized by a shallowing-upward mixed carbonate-siliciclastic sequence dominated by widespread accumulations of *Nummulites* and *Assilina* and rare orthophragmines indicating the reestablishment of the shallow-marine environmental conditions. The upper part of the sequence is more silty and marly than the lower part, displaying cyclic sedimentation. Schaub (1962) originally established *Nummulites lehneri* from the Member C (Couche 57013 in Schaub, 1981 and Couche 3a in Hottinger, 1960) and reported the occurrence of *N.* aff. *laevigatus*, *Assilina spira abrardi* and *Alveolina* aff. *levantina*, though type-level cannot precisely be located. Also, Sirel and Deveciler (2017) reported occurrences of *N. laevigatus*, *N. pinfoldi*, and *Assilina exponens* in the lower and an assemblage of *N. perforatus*, *Alveolina nuttalli*, and *Alveolina stercusmuris* in the upper part of the section, assigning a Bartonian age for the upper part of the Member C (Table 2). The Bartonian age assignment to the Member C actually relies on the study of a pebble by Deveciler (2010) in the Haymana region, which was not collected directly from the Çayraz sequence. This pebble was estimated to derive from the Çayraz Formation. Orthophragmines are not diverse in the Member C, represented only by genus *Discocyclina*. *Discocyclina spliti polatlıensis*, *D. fortisi cairazensis*, and *Discocyclina senegalensis* occur rather frequently in the lower part of this member (Özcan et al., 2007). The marly beds in the upper part of the Member C are poor in calcareous nannofossils (Figure 10) and planktonic foraminifera and do not yield key species for dating. Calcareous nannofossils belong to genera *Coccolithus*, *Chiasmolithus*, *Sphenolithus*, *Tribrachiatus*, *Ellipsolithus*, *Toweius*, *Zighrablithus*, and *Discoaster* (Figure 7).

5.1.4. Member D

This unit (approximately 40-m-thick), not described previously, is characterized by a greyish brown-colored massive marly sequence cropping out in a limited area to the northwest of Çayraz village. It is exposed along a small creek due to an NW-SE running fault where its lower boundary with carbonates and marls with abundant LBFs is nicely observed. The unit plunges to the north below the unconsolidated Quaternary clastic rocks. The Member D lacks LBFs but is rich in planktonic foraminifera and calcareous nannofossils (Figures 10, 11, 14). Calcareous nannofossils belong to *Blackites*, *Braarudosphaera*, *Campylosphaera*, *Chiasmolithus*, *Clausicoccus*, *Coccolithus*, *Cyclicargolithus*, *Dictyococcites*, *Discoaster*, *Helicosphaera*, *Lanternithus*, *Michrantolithus*, *Pemma*, *Pontosphaera*, *Pyrocyclus*, *Reticulofenestra*, *Sphenolithus*, *Umblicosphaera*, *Nannotetrina*, and *Zygrhablithus*. Assemblages of the species of the above genera indicate CNE12 Zone (NP15p.p.-NP16p.p. and CP13c zones). Planktonic foraminifera consist of the species such as *Subbotina*, *Acarinina*, *Hantkenina*, *Globigerinatheka*, *Pearsonites, Morozovelloides, Planorotalites, Pseudohastigerina, Turborotalia*, *Guembelitrioides*, and *Parasubbotina*, which suggest the E9 Zone, based on the concurrent ranges of *Globigerinatheka kugleri* and *Pearsonites* (*broedermanni* and *anapetes*).

6. Conclusion

The Çayraz Formation is subdivided into four members with distinct lithological and paleontological features. Two shelf systems (Members A and C), characterized by the common occurrence of LBF, are overlain by deep-marine marly-silty sediments (Members B and D), containing planktonic foraminifera, calcareous nannofossils and minor resedimented LBF. The uppermost part of the Eskipolatlı

Table 2. Geographic coordinates of the investigated sections.

Section	Beginning of the section	End of the Section
ÇAYA	N39°28′38.99″, E32°31′43.99″	N39°28′39.64″, E32°31′44.68″
ÇAYB	N39°29′4.68″ , E32°30′49.59″	N39°29′6.69″ , E32°30′50.62″
ÇAYC	N39°28′39.63″, E32°32′1.38″	N39°28′45.79″, E32°32′1.45″
ÇAYD	N39°28′58.82″, E32°31′55.93″	N39°28′59.43″, E32°31′56.90″
ÇAYE	N39°28′56.22″, E32°32′16.16″	N39°28′59.04″, E32°32′14.36″
ÇAYF	N39°29′1.85″, E32°32′16.95″	N39°29′2.80″, E32°32′17.00″
ÇAYG	N39°28′48.71″, E32°32′35.25″	N39°28′55.39″, E32°32′33.48″
ÇAYH	N39°29′10.30″, E32°32′15.48″	N39°29′10.74″, E32°32′14.77″

Formation containing deep-marine siliciclastic beds yields an assemblage indicating CNE3 Zone, constraining the onset of the shallow-marine sedimentation (Member A of the Çayraz Formation) to the middle Ypresian. The marly/silty beds of Member B yielded a calcareous nannofossil assemblage representing the late Ypresian CNE6 Zone, which supports previous planktonic foraminifera indicating P9 Zone. The Member C consists of carbonate siliciclastic rocks overlain by deep-marine hemipelagic marls of the Member D, which is introduced for the first time in this study. The Member D lacks LBFs but is rich in planktonic foraminifera and calcareous nannofossils. Planktonic foraminifera assemblage, represented by *Subbotina*, *Acarinina*, *Hantkenina*, *Globigerinatheka*, *Pearsonites*, *Morozovelloides*, *Planorotalites*, *Pseudohastigerina*, *Turborotalia*, *Guembelitrioides*, and *Parasubbotina* indicates E8/9 Zone and deep, relatively stable environment according to a high amount of deep-dwelling species of *Subbotina*, *Turborotalia*, *Hantkenina*, and *G. nuttalli*. Moreover, the calcareous nannofossil assemblage of the Member D characterized by *Blackites*, *Braarudosphaera*, *Campylosphaera*, *Chiasmolithus*, *Clausicoccus*, *Coccolithus*, *Cyclicargolithus*, *Dictyococcites*, *Discoaster*, *Helicosphaera*, *Lanternithus*, *Michrantolithus*, *Pemma*, *Pontosphaera*, *Pyrocyclus*, *Reticulofenestra*, *Sphenolithus*, *Umblicosphaera*, *Nannotetrina*, and *Zygrhablithus* points out CNE9-10/12 Zone thus constraining the termination age of shallow marine sedimentation. We conclude that shallow-marine sedimentation in the Çayraz section ended in the 'middle' Lutetian, challenging the previous Bartonian records by LBFs.

Acknowledgments

This work was part of Ali Osman Yücel's PhD Thesis and realized within the project 'Paleocene-Eocene Planktonic foraminifera from deep-marine deposits with resedimented larger benthic foraminifera in several Anatolian basins (Thrace, Haymana, Karabük basins and western Taurides)' supported by the BAP unit of İstanbul Technical University (Project ID: MDK-2019-42499).

References

Agnini C, Fornaciari E, Raffi I, Catanzariti R, Pälike H et al. (2014). Biozonation and biochronology of Paleogene calcareous nannofossils from low and middle latitudes. Newsletters on Stratigraphy 47 (2): 131-181.

Agnini C, Fornaciari E, Rio D, Tateo F, Backman J et al. (2007). Responses of calcareous nannofossil assemblages, mineralogy and geochemistry to the environmental perturbations across the Paleocene/Eocene boundary in the Venetian Pre-Alps. Marine Micropaleontology 63: 19-38.

Agnini C, Muttoni G, Kent DV, Rio D (2006). Eocene biostratigraphy and magnetic stratigraphy from Possagno, Italy: the calcareous nannofossil response to climate variability. Earth and Planetary Science Letters 241: 815-830.

Angori E, Bernaola G, Monechi S (2007). Calcareous nannofossil assemblages and their response to the Paleocene-Eocene thermal Maximum event at different latitudes: ODP Site 690 and Tethyan sections, in: large Ecosystem Perturbations: Causes and Consequences. Geological Society of America. https://doi.org/10.1130/ 2007.2424(04).

Armstrong H, Brasier M (2005). Microfossils. Blackwell Publishing, pp. 296.

Aubry M-P (1992). Late Paleogene Calcareous Nannoplankton Evolution: A Tale of Climatic Deterioration, in: Prothero, D.R., Berggren, W.A. (Eds.), Eocene-Oligocene Climatic and Biotic Evolution. Princeton University Press, Princeton. pp 272-309.

Aubry M-P (1998). Early Paleogene calcareous nannoplankton evolution: a tale of climatic amelioration. In: Aubry M-P, Lucas S, Berggren W (Eds.), Late Paleocene–early Eocene Climatic and Biotic Events in the Marine and Terrestrial Record. Columbia University Press, 158-203.

Berggren WA, Pearson PN, Huber BT, Wade BS (2006). Taxonomy, biostratigraphy, and phylonegy of Eocene Acarinina. In: Pearson PN, Olsson RK, Huber BT, Hemleben C, Berggren WA (Eds.), Atlas of Eocene Planktonic Foraminifera. Cushman Foundation Special Publications 41: 257-326.

Berggren WA, Kent DV, Swisher III CC, Aubry M-P (1995). A revised Cenozoic geochronology and chronostratigraphy. In: Berggren WA, Kent DV, Aubry M-P, Hardenbol J (Eds.), Geochronology, Time Scales and Global Stratigraphic Correlation. SEPM Special Publications 54: 129-212.

Berggren WA, Pearson PN (2005). A revised tropical to subtropical Paleogene planktonic foraminiferal zonation. Journal of Foraminiferal Research 35: 279-298.

Boersma A, Premoli Silva I, Shackleton N (1987). Atlantic Eocene planktonic foraminiferal biogeography and stable isotopic paleoceanography. Paleoceanography 2: 287-331.

Bown PR, Lees JA, Young JR (2004). Calcareous nannoplankton evolution and diversity through time. In: Thierstein HR, Young JR (Eds.), Coccolithophores - from molecular processes to global impact, London. Springer-Verlag, 481-505.

Bown PR, Young JR (1999). Techniques. In: Bown PR (Ed.), Calcareous Nannofossil Biostratigraphy: 16-28. British Micropalaeontology Society Publication Series. Kluwer Academic Publishers, Dordrecht.

Bralower TJ (2002). Evidence of surface water oligotrophy during the Paleocene-Eocene thermal maximum: Nannofossil assemblage data from Ocean Drilling Program Site 690, Maud Rise, Weddell Sea. Paleoceanography 17: PA000662.

Bramlette MN, Martini E (1964). The great change in calcareous nannoplankton fossils between the Maestrichtian and the Danian. Micropaleontology 10:291-322.

Bukry D (1973). Low-latitude coccolith biostratigraphic zonation. In: Edgar NT, Saunders JB (Eds.), Proceedings of the Ocean Drilling Program, Initial Reports, Ocean Drilling Program. College Station, TX, USA, 15: 685-703.

Bukry D (1981). Pacific Coast Coccolith Stratigraphy between Point Conception and Cabo Corrientes, Deep Sea Drilling Project Leg 63, In: initial reports of the Deep Sea Drilling Project 63: 445-471.

Bybell LM, Gartner S (1972). Provincialism among mid-Eocene calcareous nannofossils. Micropaleontology 18: 319-336.

Çiner A, Deynoux M, Koşun E (1996a). Cyclicity in the Yamak turbidite complex of Haymana basin Turkey. Geologische Rundschau 85: 669-682.

Çiner A, Deynoux M, Koşun E, Gündoğdu N (1993). Beldede Örgülü-Delta Karmaşığı'nın (BÖDK) sekans stratigrafik analizi: Polatlı-Haymana baseni (Orta Eosen), Orta Anadolu. Bulletin for Earth Sciences 16: 67-92.

Çiner A, Deynoux M, Ricou S, Koşun E (1996b). Cyclicity in the Middle Eocene Çayraz carbonate formation, Haymana basin, Central Anatolia, Turkey. Palaeogeography, Palaeoclimatology, Palaeoecology 121: 313-329.

Deveciler A (2010). The first appearance of the Bartonian benthic foraminifera at the Çayraz section (north of Haymana, south Ankara, central Turkey). Bulletin for Earth Sciences 31: 191-203.

Dizer A (1964). Sur quelques Alveolines de l'Eocene de Turquie. Revue de Micropaleontologie 7 (4): 265-279.

Dizer A (1968). Étude Micropaléontologique du Nummulitique de Haymana (Turquie). Revue de Micropaleontologie 11 (1): 13-21.

Dunkley Jones T, Bown PR, Pearson PN, Wade BS, Coxall HK et al. (2008). Major shifts in calcareous phytoplankton assemblages through the Eocene-Oligocene transition of Tanzania and their implications for low-latitude primary production. Paleoceanography 23: PA4204.

Edwards AR (1968). The calcareous nannoplankton for Tertiary New Zealand climates. Tuatara 16: 26–31.

Edwards AR, Perch-Nielsen K (1975). Calcareous nannofossils from the southern southwest Pacific, Deep Sea Drilling Project, Leg 29. In: Kennett JP, Houtz RE et al., 1975, Initial Reports of the Deep Sea Drilling Project, 29. U.S. Government Printing Office, Washington, D.C. 469-539.

Gradstein FM, Ogg JG, Schmitz MD, Ogg GM (2012). The geologic time scale 2012. Elsevier.

Gibbs SJ, Bown PR, Sessa JA, Bralower TJ, Wilson PA (2006). Nannoplankton Extinction and Origination across the Paleocene-Eocene Thermal Maximum. Science 314: 1770-1773.

Giorgioni M, Jovane L, Rego ES, Rodelli D, Frontalini F et al. (2019). Carbon cycle instability and orbital forcing during the Middle Eocene Climatic Optimum. Scientific Reports 9: 9357.

Haq BU, Lohmann GP (1976). Early Cenozoic calcareous nannoplankton biogeography of the Atlantic Ocean. Marine Micropaleontology 1: 120-197.

Hottinger L (1960). Recherches sur les Alveolines du Paleocene et de l'Eocene. Abhandlungen der Schweizerischen Palaeontolosichen 75-76: 1-243.

Kalb AL, Bralower TJ (2012). Nannoplankton origination events and environmental changes in the late Paleocene and early Eocene. Marine Micropaleontology 92-93: 1-15.

Kleijne A (1991). Holooccoliphorids from the Indian Ocean, Red Sea, Mediterranean and North Atlantic Ocean. Marine Micropaleontology 17: 1-76.

Koçyiğit A (1991). An example of an accretionary forearc basin from Central Anatolia and its implications for the history of subduction of Neo-Tethys in Turkey. Geological Society of America 103: 22-36.

Luciani V, Giusberti L, Agnini C, Fornaciari E, Rio D et al. (2010). Ecological and evolutionary response of Tethyan planktonic foraminifera to the middle Eocene climatic optimum (MECO) from the Alano section (NE Italy). Palaeogeography, Palaeoclimatology, Palaeoecology 292: 82-95.

Martini E (1971). Standard Tertiary and Quaternary calcareous nannoplankton zonation. In: Farinacci A (Ed.), Proceedings of the Second Planktonic Conference Roma, 2: 739-785. Edizioni Tecnoscienza, Roma.

Müller C (1976). Tertiary and Quaternary calcareous nannoplankton in the Norwegian-Greenland Sea, D.S.D.P. leg 38. In: Talwani M, Udintsev G et al. (1976), Initial Reports of the Deep Sea Drilling Project, 38. U.S. Government Printing Office, Washington, D.C., 823-841.

Monechi S, Buccianti A, Gardin S (2000). Biotic signals from nannoflora across the iridium anomaly in the upper Eocene of the Massignano section: Evidence from statistical analysis. Marine Micropaleontology 39: 219-237.

Okada H, Bukry D (1980). Supplementary modification and introduction of code numbers to the low–latitude coccolith biostratigraphy zonation (Bukry 1973; 1975). Marine Micropaleontology 5: 321-325.

Okay AI, Altıner D (2016). Carbonate sedimentation in an extensional active margin: Cretaceous history of the Haymana region, Pontides. International Journal of Earth Sciences 105: 2013-2030.

Okay AI, Tüysüz O (1999). Tethyan sutures of northern Turkey. In: Durand B, Jolivet L, Horwáth F, Séranne M (Eds.) The Mediterranean Basins: Tertiary extension within the Alpine Orogen. Geological Society 156: 475-515.

Okay AI, Zattin M, Özcan E, Sunal G (2020). Uplift of Anatolia. Turkish Journal of Earth Sciences 29: 696-713.

Özcan E (2002). Cuisian orthophragminid assemblages (*Discocyclina*, *Orbitoclypeus*, *Nemkovella*) from Haymana-Polatlı basin (central Turkey): biometry and description of two new taxa. Eclogae geologicae Helvetiae 95: 75-97.

Özcan E, Çiner A, Soussi M, Hakyemez A, Okay AI et al. (2018). Eocene Çayraz Formation (Haymana Basin) revisited: an integrated foraminiferal paleontology and sedimentology and age constraints based on new planktonic foraminiferal data. Proceedings of 71th Geological Congress of Turkey.

Özcan E, Hakyemez A, Çiner A, Okay AI, Soussi M et al. (2020) Reassessment of the age and depositional environments of the Eocene Çayraz Formation; a reference unit for Tethyan larger benthic foraminifera (Haymana basin, Central Turkey). Journal of Asian Earth Sciences 193: 104304

Özcan E, Less G, Kertesz B (2007). Late Ypresian to middle Lutetian orthophragminid record from central and northern Turkey: taxonomy and remarks on zonal scheme. Turkish Journal of Earth Sciences 16: 281-321.

Özcan E, Sirel E, Özkan-Altıner S, Çolakoğlu S (2001). Late Paleocene Orthophragminae (Foraminifera) from the Haymana–Polatlı Basin (Central Turkey) and description of a new taxon, *Orbitoclypeus haymanaensis*. Micropaleontology 47: 339-357.

Özcan E, Yücel AO, Erkızan LS, Gültekin MN, Kayğılı S et al. (2022). Atlas of Tethyan orthophragmines. Mediterranean Geoscience Reviews 4 (1): 3-213.

Papazzoni CA, Ćosović V, Briguglio A, Drobne K (2017). Towards a calibrated larger Foraminifera biostratigraphic zonation: Celebrating 18 years of the application of Shallow Benthic Zones. Palaios 32(1): 1-5.

Pearson PN, Ditchfield PW, Singano J, Harcourt-Brown KG, Nicholas CJ, Olsson RK, Shackleton NJ, Hall MA (2001). Warm tropical sea surface temperatures in the Late Cretaceous and Eocene epochs. Nature 413: 481-487.

Pearson PN, Olsson RK, Huber BT, Hemleben C, Berggren WA (2006). Atlas of Eocene planktonic foraminifera. Cushman Foundation for Foraminiferal Research Special Publication 41, Fredericksburg, USA.

Pearson PN, Shackleton NJ, Hall MA (1993). Stable isotope paleoecology of middle Eocene planktonic foraminifera and integrated isotope stratigraphy, DSDP Site 523, South Atlantic. Journal of Foraminiferal Research 23: 123-140.

Perch-Nielsen K (1985). Cenozoic calcareous nannofossils. In: Bolli HM, Saunders JB, Perch-Nielsen K (Eds.), Plankton Stratigraphy. Cambridge University Press, 427-554.

Persico D, Villa G (2004). Eocene–Oligocene calcareous nannofossils from Maud Rise and Kerguelen Plateau (Antarctica): paleoecological and paleoceanographic implications. Marine Micropaleontology 52: 153-179.

Schaub H (1981). Nummulites et Assilines de la Tethys Paléogène. Taxonomie, phylogénèse et biostratigraphie. Abhandlungen der Schweizerischen Palaeontolosichen 104-106: 236.

Schneider LJ, Bralower TJ, Kump LR (2011). Response of nannoplankton to early Eocene Ocean destratification. Palaeogeography, Palaeoclimatology, Palaeoecology 310: 152-162.

Self-Trail JM, Powars DS, Watkins DK, Wandless G (2012). Calcareous nannofossil assemblage changes across the Paleocene-Eocene thermal maximum: Evidence from a shelf setting. Marine Micropaleontology 92-93: 61-80.

Serra-Kiel J, Hottinger L, Caus E, Drobne K, Ferràndez C et al. (1998). Larger foraminiferal biostratigraphy of the Tethyan Paleocene and Eocene. Bulletin de la Société Géologique de France 169: 281-299.

Siesser WG, Bralower TJ, De Carlo EH (1992). Mid-Tertiary Braarudosphaera-rich sediments on the Exmouth Plateau. Proceedings of the Ocean Drilling Program Scientific results 122: 653-663.

Sirel E (1992). Field Trip. In: Introduction to the early Paleogene of the Haymana-Polatlı Basin, IGCP 286 'Early Paleogene Benthos'. Third Meeting, Ankara (Turkey), General Directory of Mineral Research and Exploration. 1-10.

Sirel E (1975). Polatlı (GB Ankara) güneyinin stratigrafisi. Bulletin of the Geological Society of Turkey 18: 181-192.

Sirel E (1998). Foraminiferal description and biostratigraphy of the Paleocene- Lower Eocene shallow-water limestones and discussion on the Cretaceous-Tertiary boundary in Turkey, General Directorate of the Mineral Research and Exploration Monography Series. No: 2.

Sirel E (1999). Four new genera (*Haymanella*, *Kayseriella*, *Elazıgella* and *Orduella*) and one new species of *Hottingerina* from the Paleocene of Turkey. Micropaleontology 45: 113-137.

Sirel E (2009). Reference sections and key localities of the Paleocene Stages and their very shallow/shallow-water three new benthic foraminifera in Turkey. Revue de Paleobiologie 28: 413-435.

Sirel E, Acar Ş (2008). Description and biostratigraphy of the Thanetian-Bartonian Glomalveolinids and Alveolinids of Turkey. UCTEA The Chamber of Geological Engineers Publication: 103.

Sirel E, Deveciler A (2017). A new late Ypresian species of *Asterigerina* and the first records of *Ornatorotalia* and *Granorotalia* from the Thanetian and upper Ypresian of Turkey. Rivista Italiana di Paleontologia e Stratigrafia 123: 65-78.

Sirel E, Gündüz H (1976). Description and stratigraphical distribution of some species of the genera *Nummulites*, *Assilina* and *Alveolina* from the Ilerdian, Cuisian and Lutetian of Haymana region (S Ankara). Bulletin of the Geological Society of Turkey 19: 31-44.

Toker V (1980). Haymana yöresi (GB Ankara) nannoplankton biyostratigrafisi. Bulletin of the Geological Society of Turkey 23: 165-178.

Tremolada F, Bralower TJ (2004). Nannofossil assemblage fluctuations during the Paleocene–Eocene thermal Maximum at Sites 213 (Indian Ocean) and 401 (North Atlantic Ocean): palaeoceanographic implications. Marine Micropaleontology 52: 107-116.

Ünalan G, Yüksel V, Tekeli T, Gönenç O., Seyirt Z et al. (1976). Haymana-Polatlı yöresinin (GB Ankara) Üst Kretase- Alt Tersiyer stratigrafisi ve paleocoğrafik evrimi. Geological Bulletin of Turkey 19: 159-176.

Villa G, Fioroni C, Pea L, Bohaty S, Persico D (2008). Middle Eocene–late Oligocene climate variability: Calcareous nannofossil response at Kerguelen Plateau, Site 748. Marine Micropaleontology 69: 173-192.

Wade BS, Pearson PN, Berggren WA, Pälike H (2011). Review and revision of Cenozoic tropical planktonic foraminiferal biostratigraphy and calibration to the geomagnetic polarity and astronomical time scale. Earth-Science Reviews 104: 111-142.

Wei W, Wise SW (1990). Biogeographic gradients of middle Eocene-Oligocene calcareous nannoplankton in the South Atlantic Ocean. Palaeogeography, Palaeoclimatology, Palaeoecology 79: 29-61.

Wei W, Villa G, Wise SWJ (1992). Paleoceanographic Implications of EoceneOligocene Calcareous Nannofossils from Sites 711 and 748 in the Indian Ocean, in: Proceedings of the Ocean Drilling Program, 120 Scientific results. Ocean Drilling Program.

Westerhold T, Röhl U, Donner B, Zachos JC (2018). Global extent of early Eocene hyperthermal events: A new Pacific benthic foraminiferal isotope record from Shatsky Rise (ODP Site 1209). Palaeogeography, Palaeoclimatology, Palaeoecology 33: 626-642.

Table S1. Quantitative distribution of calcareous nannofossils in the section ÇAYA.

ÇAYA SECTION	Total abundance	Total abundance of reworked forms	Numbers in %												Numbers on 100 FOV						Zone	Age
			Chiasmolithus+ *ruciplacolithus*	*C. fenestratus*	*C. pelagicus*	*Discoaster spp.*	*Ellipsolithus spp.*	*Spenolithus spp.*	*T. callosus*	*T. occultatus*	*T. pertusus*	*T. rotundus*	*Toweius sp.*	*Z. bijugatus*	*D. barbadiensis*	*D. binodosus*	*D. diastypus*	*D. gemmifer*	*Discoaster sp.*	*T. orthostylus*		
ÇAYA5	F	F	1.0	1.0	20.0	1.0	1.0	17.0	5.0	0.0	39.0	3.0	4.0	8.0	3	0	0	0	1	1	CNE3-NP10p.p./ NP11-CP9b	Ypresian-early Eocene
ÇAYA4	F	F	0.0	0.0	27.0	1.0	1.0	22.0	7.0	0.0	34.0	1.0	4.0	4.0	0	0	0	1	0	0		
ÇAYA3	F	R	0.0	0.0	36.0	1.0	0.0	21.0	6.0	1.0	25.0	6.0	0.0	4.0	0	0	0	0	1	1		
ÇAYA2	F	F	1.0	0.0	30.0	1.0	1.0	13.0	3.0	3.0	40.0	5.0	2.0	1.0	0	2	2	0	2	2		
ÇAYA1	F	F	1.0	0.0	35.0	0.0	0.0	11.0	4.0	2.0	40.0	4.0	3.0	0.0	0	0	0	0	0	0		

Table S2. Quantitative distribution of calcareous nannofossils in the section ÇAYB.

ÇAYB SECTION	Total abundance	Total abundance of reworked forms	Numbers on 100 FOV														Zone	Age
			Chiasmolithus sp.	*C. formosus*	*C. pelagicus*	*D. barbadiensis*	*D. kuepperi*	*D. multiradiatus*	*T. gammation (primitive)*	*Spenolithus* spp.	*S. editus*	*S. radians*	*S. villae*	*T. callosus*	*T. pertusus*	*T. orthostylus*	*Z. bijugatus*		
ÇAYB7	R	F	0	0	0	0	0	0	0	0	0	0	0	0	0	0	0	CNE3-NP11/CP9b	Ypresian-early Eocene
ÇAYB6	R	F	0	0	4	0	0	0	0	2	1	0	cf	2	1	0	0		
ÇAYB5	R	F	0	0	5	0	0	0	0	2	0	1	0	0	0	0	0		
ÇAYB4	R	R	1	0	20	1	2	0	0	8	1	4	0	6	0	0	0		
ÇAYB3	R	F	1	0	9	0	0	0	0	2	0	1	0	0	0	0	0		
ÇAYB2	R	F	2	1	26	0	2	1	4	18	0	6	0	22	2	1	4		
ÇAYB1	R	F	0	0	18	0	0	0	0	21	1	0	0	18	0	0	6		

Table S3. Quantitative distribution of calcareous nannofossils in the section ÇAYC.

ÇAYC SECTION	Total abundance		Total abundance of reworked forms	Numbers in %															Numbers on 100 FOV																		Zone	Age
				Chiasmolithus spp.	Chiphragmalithus spp.	Clausicoccus sp.	Coccolithus crassus	C. formosus	C. pelagicus	C. floridanus	Dictyococcites sp.	Discoaster sp.	T. gammation	Helicosphaera spp.	L. minutus	P. inversus	R. dictyoda	S. orphanknollensis	S. radians	Sphenolithus spp.	Z. bijugatus	B. gladius	Camptosphaera dela	Chiasmolithus grandis	C. nitidus+titus	C. solitus	Chiasmolithus sp.	D. barbadiensis	D. deflandrei	D. kuepperi	D. lodoensis	D. nodifer	D. nonaradiatus	D. saipanensis	D. subloduensis	Discoaster sp.	H. lophota	H. seminulum	Micrantholithus	U. protoannulus	
ÇAYC35	R	F	0.0	0.0	0.0	0.0	0.0	10.0	43.0	20.0	0.0	0.0	0.0	0.0	0.0	0.0	10.0	1.0	10.0	5.0	0	0	0	0	0	0	0	0	0	0	0	0	0	0	0	0	0	1	CNE6-NP14p.p.-CP12ap.p.	late Ypresian-early Eocene
ÇAYC34	F	R	0.6	0.0	0.6	0.0	0.0	11.0	17.0	32.8	0.0	2.0	0.0	0.0	2.0	0.0	15.0	3.0	5.0	9.0	2.0	0	0	1	1	0	0	8	0	0	1	0	0	0	2	0	1	0	0	0	1	
ÇAYC33	F	F	1.0	0.3	0.3	0.3	0.0	10.0	18.0	18.0	0.0	6.5	0.3	0.0	0.3	0.0	16.0	5.0	6.0	14.0	4.0	0	0	0	3	0	0	6	0	2	1	0	1	6	1	0	2	0	0	0	0	
ÇAYC32	R	R	0.0	0.0	0.0	0.0	0.0	12.0	40.0	20.0	0.0	3.0	0.6	0.0	0.0	0.0	13.5	0.6	0.0	10.0	0.3	0	0	0	0	0	0	3	0	0	0	0	0	2	0	2	0	0	0	0	0	
ÇAYC31	R	R	0.6	0.0	2.0	0.0	0.0	24.0	10.0	20.0	0.0	3.0	1.0	0.0	0.0	0.0	12.0	0.0	0.0	21.0	6.0	0	1	0	0	0	1	0	0	0	0	0	0	2	0	1	0	0	0	0	0	
ÇAYC30	F	R	0.0	0.3	0.0	0.0	0.0	14.0	16.0	28.0	0.6	6.0	0.0	0.0	0.0	0.0	8.0	0.0	6.0	6.0	12.0	0	0	0	0	0	0	1	0	0	0	0	0	0	0	2	0	0	0	0	0	
ÇAYC29	F	R	0.0	0.0	0.0	0.0	0.0	4.0	2.0	67.5	0.0	1.0	0.6	0.0	0.0	0.0	10.0	0.6	1.3	12.0	1.0	0	0	0	0	0	0	2	0	0	1	0	0	0	1	2	0	0	0	0	0	
ÇAYC28	F	R	0.3	0.3	0.0	0.0	0.0	6.0	10.0	34.0	0.3	1.3	2.0	0.0	0.0	0.0	33.0	3.0	3.0	4.8	2.0	0	0	0	0	0	0	1	0	0	0	0	0	4	0	4	0	0	0	0	0	
ÇAYC27	F	C	0.0	0.0	0.0	0.0	0.0	4.0	6.0	62.0	0.3	2.0	2.0	0.0	0.0	0.0	10.0	2.0	3.0	4.0	5.0	0	0	0	0	0	0	3	1	0	0	0	0	1	0	1	0	0	0	0	0	
ÇAYC26	F	R	0.0	0.0	0.0	0.0	0.0	4.0	14.0	33.0	0.0	4.0	4.0	0.0	0.0	0.0	7.0	2.0	3.0	20.0	9.0	0	0	0	0	0	0	9	1	0	1	0	0	1	0	1	0	0	0	0	0	
ÇAYC25	F	F	0.0	0.0	0.0	0.0	0.0	10.0	18.0	40.3	0.0	0.3	0.0	1.0	0.0	0.0	12.0	0.0	0.0	16.3	2.0	0	0	0	0	0	0	1	0	0	0	0	0	2	0	0	2	1	0	0	0	
ÇAYC24	F	F	0.6	0.0	0.0	0.0	0.0	3.0	8.0	40.3	0.0	0.6	0.3	0.0	0.0	0.0	30.0	0.0	0.3	11.6	5.0	0	1	0	0	0	0	3	0	0	0	0	0	1	2	1	3	0	0	0	0	
ÇAYC23	F	F	0.0	0.0	0.0	0.0	0.0	4.0	16.0	39.5	0.0	0.6	0.3	0.0	0.0	0.0	33.0	0.0	0.0	1.0	5.0	0	0	0	0	0	0	2	0	0	0	0	0	1	0	0	3	0	0	0	2	
ÇAYC22	F	R	0.3	0.0	0.0	0.0	0.0	5.0	6.0	41.0	0.0	0.0	0.0	0.3	0.0	0.3	24.9	0.6	0.6	15.0	6.0	0	0	0	1	0	0	5	0	0	0	0	0	0	0	0	1	0	0	0	0	
ÇAYC21	F	F	0.0	0.0	0.0	0.0	0.0	8.0	5.0	42.0	0.0	0.6	0.3	0.0	0.3	0.0	24.0	0.6	0.6	15.6	3.0	0	0	0	0	0	0	2	0	1	0	0	0	0	0	0	0	0	0	0	0	
ÇAYC20	F	R	0.0	0.0	0.0	0.0	0.0	6.0	15.0	45.0	0.0	0.0	6.0	0.0	0.0	0.0	11.0	1.0	4.0	11.0	1.0	0	0	0	1	0	0	6	0	0	0	0	0	2	1	0	0	0	0	0	0	
ÇAYC19	F	F	0.6	0.0	0.0	0.0	0.0	14.0	10.0	37.0	0.3	1.0	0.0	0.3	0.0	0.0	21.0	0.6	1.0	6.0	8.0	0	1	0	0	0	0	9	0	0	1	0	1	0	0	1	0	0	0	0	0	
ÇAYC18	F	F	0.0	0.0	0.0	0.0	0.0	13.0	5.0	38.0	0.0	0.0	0.0	0.0	0.0	0.0	30.0	0.0	1.0	12.0	1.0	0	0	0	0	0	0	0	0	0	0	0	0	0	0	0	0	0	0	0	0	
ÇAYC17	F	F	0.0	0.0	0.0	0.0	0.0	7.0	14.0	49.0	0.0	1.0	1.0	1.0	1.0	0.0	14.0	1.0	2.0	5.0	4.0	0	0	0	0	0	0	3	0	0	0	cf	0	0	4	0	2	0	0	0	0	
ÇAYC16	R	F	0.0	0.0	0.0	0.0	0.0	12.0	18.0	34.0	0.0	1.0	4.0	0.0	0.0	0.0	10.0	0.0	1.0	18.0	2.0	0	0	0	0	0	0	0	1	0	1	0	0	0	0	0	0	0	0	0	0	
ÇAYC15	NC	F	0.0	0.0	0.0	0.0	0.0	P	P	P	0.0	P	0.0	0.0	0.0	0.0	P	0.0	0.0	P	0.0	0	0	0	0	0	0	3	0	0	0	0	0	0	0	0	0	0	0	0	0	
ÇAYC14	NC	F	0.0	0.0	0.0	0.0	0.0	P	P	P	0.0	0.0	0.0	0.0	0.0	0.0	P	0.0	0.0	P	0.0	0	0	0	0	0	0	0	0	0	0	0	0	0	0	0	0	0	0	0	0	
ÇAYC13	NC	F	0.0	0.0	0.0	0.0	0.0	0.0	0.0	0.0	0.0	0.0	0.0	0.0	0.0	0.0	0.0	0.0	0.0	0.0	0.0	0	0	0	0	0	0	0	0	0	0	0	0	0	0	0	0	0	0	0	0	
ÇAYC12	NC	F	0.0	0.0	0.0	0.0	0.0	P	P	P	0.0	0.0	0.0	0.0	0.0	0.0	0.0	0.0	0.0	P	0.0	0	0	0	0	0	0	0	0	0	0	0	0	0	0	0	0	0	0	0	0	
ÇAYC10	F	C	0.0	0.0	0.6	0.0	0.0	11.4	15.0	30.0	0.0	1.0	1.0	0.0	0.0	0.0	12.0	2.0	3.0	20.0	4.0	0	0	0	0	0	0	5	0	0	1	0	1	1	0	2	0	0	0	0	0	
ÇAYC7	F	F	0.0	0.0	0.3	0.0	0.0	5.0	7.0	46.0	0.0	0.6	2.0	0.3	0.3	0.6	15.0	0.0	2.0	13.9	7.0	0	0	0	0	0	0	5	0	0	2	0	1	0	0	2	1	0	0	0	0	
ÇAYC5	F	F	0.0	0.0	0.0	0.0	0.0	8.0	14.0	39.0	0.0	2.0	4.0	0.0	0.0	0.0	7.0	1.0	7.0	14.0	4.0	0	0	0	0	0	0	3	1	2	1	1	1	0	0	2	0	0	0	0	0	
ÇAYC3	NC	F	0.0	0.0	0.0	0.0	0.0	0.0	P	0.0	0.0	0.0	0.0	0.0	0.0	0.0	0.0	0.0	0.0	0.0	0.0	0	0	0	0	0	0	0	0	0	0	0	0	0	0	0	0	0	0	0	0	
ÇAYC2	F	F	0.0	0.0	1.0	1.3	5.0	14.0	39.0	0.0	2.0	1.3	1.3	0.3	0.0	7.3	0.6	0.3	10.6	16.0	0	0	0	0	0	0	16	3	0	4	1	1	1	2	3	0	0	0	1		
ÇAYC1	F	F	0.6	0.3	0.6	1.6	10.0	15.0	37.0	0.0	2.0	1.3	1.0	0.0	0.0	5.6	0.0	11.0	10.0	4.0	1	0	2	0	0	0	0	4	0	4	2	0	0	2	0	1	2	1	3	0	

Table S4. Quantitative distribution of calcareous nannofossils in the section ÇAYD.

ÇAYD SECTION	Total abundance	Total abundance of reworked forms	Numbers on 100 FOV				Zone	Age
			C. formosus	*C. pelagicus*	*Discoaster* sp.	*R. dictyoda*		
ÇAYD3	Barren		0	0	0	0	?	late Ypresian-lower Lutetian
ÇAYD2	Barren		0	0	0	0		
ÇAYD1	R	R	1	1	1	10		

Table S5. Quantitative distribution of calcareous nannofossils in the section ÇAYE.

ÇAYE SECTION	Total abundance	Total abundance of reworked forms	Numbers in %											Zone	Age
			C. formosus	*C. pelagicus*	*C. floridanus*	*Dictyococcites* sp.	*D. barbadiensis*	*D. kuepperi*	*Discoaster* sp.	*H. seminulum*	*L. minutus*	*R. dictyoda*	*S. radians*	*Sphenolithus* spp.	
ÇAYE12	R	R	5.0	20.0	56.0	0.0	3.0	0.0	P	0.0	0.0	13.0	0.0	3.0	?	late Ypresian-lower Lutetian early-middle Eocene
ÇAYE11	R	R	13.0	20.0	47.0	0.0	P	0.0	P	0.0	0.0	7.0	0.0	13.0		
ÇAYE10	R	R	7.0	10.0	67.0	0.0	0.0	0.0	0.0	0.0	0.0	7.0	3.0	6.0		
ÇAYE9	F	R	5.0	24.0	52.0	0.0	2.0	P	P	1.0	0.0	12.0	0.0	4.0		
ÇAYE8	R	R	11.0	9.0	57.0	1.0	P	0.0	P	0.0	2.0	12.0	1.0	7.0		
ÇAYE7	R	R	3.0	4.0	70.0	0.0	0.0	0.0	0.0	0.0	0.0	0.0	3.0	20.0		
ÇAYE6	R	R	5.0	15.0	54.0	1.0	0.0	P	0.0	0.0	0.0	5.0	0.0	20.0		
ÇAYE5	R	R	10.0	10.0	40.0	0.0	0.0	0.0	0.0	0.0	0.0	30.0	5.0	5.0		
ÇAYE4	R	R	20.0	10.0	50.0	0.0	P	0.0	0.0	0.0	0.0	15.0	0.0	5.0		
ÇAYE3	R	R	10.0	0.0	70.0	0.0	0.0	0.0	0.0	0.0	0.0	10.0	0.0	10.0		
ÇAYE2	Barren		0.0	0.0	0.0	0.0	0.0	0.0	0.0	0.0	0.0	0.0	0.0	0.0		
ÇAYE1	R	R	0.0	50.0	30.0	0.0	0.0	0.0	0.0	0.0	0.0	0.0	0.0	20.0		

Table S6. Quantitative distribution of calcareous nannofossils in the section ÇAYF.

ÇAYF1	ÇAYF2	ÇAYF3	ÇAYF4	ÇAYF5	ÇAYF6	ÇAYF7	ÇAYF8	ÇAYF9	ÇAYF10	**ÇAYF** SECTION
F	F	F	A	F	F	A	A	A	A	Total abundance
R	R	R	R	/	R	/	/	R	/	Total abundance of reworked forms
0.3	0.6	0.0	0.3	0.0	0.3	0.3	0.6	0.3	0	*Chiasmolithus* spp.
0.0	0.3	0.0	0.3	0.3	0.3	0.3	0.6	0.6	0.3	*Clausicoccus* spp.
2.0	8.0	2.0	1.3	6.0	5.0	3.3	1.3	2.0	2.6	*C. formosus*
4.0	3.0	2.0	2.0	1.0	4.0	1.0	1.6	4.0	2.3	*C. pelagicus*
57.0	51.3	55.0	53.6	50.0	56.0	51.0	57.6	58.0	50.0	*C. floridanus*
0.0	0.0	0.0	0.0	0.3	0.0	0.0	0.0	0.6	0.6	*Dictyococcites* sp.
1.0	1.0	1.3	1.3	2.6	3.3	3.3	1.6	2.3	1.0	*Discoaster* spp.
0.3	0.0	0.0	0.0	0.3	0.0	0.3	0.6	0.0	0.3	*Helicosphaera* spp.
1.3	0.3	0.6	0.0	2.0	0.0	2.3	4.0	2.3	3.0	*L. minutus*
0.3	0.3	0.6	1.0	0.6	1.0	0.6	0.3	1.0	1.0	*Pemma* spp.
0.3	0.3	0.6	0.3	0.0	0.3	1.3	0.6	1.3	1.0	*P. inversus*
30.0	31.0	28.0	22.0	27.0	26.3	27.0	24.0	20.0	27.0	*R. dictyoda*
3.0	3.3	8.0	13.0	5.0	3.0	7.0	5.0	6.0	8.3	*Sphenolithus* spp.
0.3	0.6	2.0	5.0	5.0	0.3	2.3	2.0	1.6	2.6	*Z. bijugatus*
100.0	78.0	70.0	70.0	60.0	76.0	68.0	66.0	62.0	60.0	*Sphenolithus* sp.
0.0	2.0	6.0	2.0	6.0	9.0	10.0	16.0	10.0	2.0	*S. perpendicularis*
0.0	0.0	0.0	2.0	0.0	0.0	2.0	0.0	2.0	2.0	*S. radians*
0.0	10.0	24.0	26.0	34.0	15.0	20.0	18.0	26.0	36.0	*S. spiniger*
0	0	0	0	1	0	0	1	2	1	*B. gladius*
1	2	1	1	1	1	1	2	1	1	*B. perampla*
0	1	2	1	1	2	1	2	1	1	*B. sequela*
0	0	0	0	1	1	0	0	0	0	*C. dela*
0	0	0	1	0	0	2	1	2	0	*C. grandis*
1	1	0	0	0	0	0	0	1	3	*C. nitidus+titus*
0	0	0	0	0	0	1	5	3	2	*C. solitus*
0	1	1	0	0	1	0	0	1	0	*Chiasmolithus* sp.
0	0	0	0	0	0	0	1	1	0	*C. mutatus*
0	0	0	0	0	0	0	1	0	0	*C. opdikey*
3	5	2	11	9	8	7	8	10	9	*D. barbadiensis*
0	1	1	0	0	2	1	2	5	1	*D. deflandrei*
1	0	0	2	0	0	0	0	0	0	*D. sept-nonaradiatus*
1	1	2	3	5	1	2	1	3	2	*D. saipanensis*
0	0	1	0	0	0	0	0	0	0	*D. tanii*
1	3	3	4	1	2	1	2	1	3	*Discoaster* sp.
	0	0	0	0	1	2	2	0	2	*H. lophota*
1	0	0	0	2	0	1	1	0	2	*H. sheminulum*
0	0	1	0	0	0	1	0	2	0	*Micrantholithus*
0	0	0	0	0	0	0	0	1	0	*N. cristata*
0	1	0	0	0	0	0	0	1	1	*N. alata/fulgens*
1	5	6	4	5	7	10	8	6	5	*Pemma* spp.
0	0	1	0	1	0	0	0	0	0	*P. versa*
0	0	0	0	0	0	3	0	0	0	*U. protoannulus*
CNE9-NP15p.p.-CP13a										Zone
Lutetian-middle Eocene										Age

Numbers in %

Numbers in %

Numbers on 100 FOV

Table S7. Quantitative distribution of calcareous nannofossils in the section ÇAYG.

ÇAYG1	ÇAYG2	ÇAYG3	ÇAYG4	ÇAYG5	ÇAYG6	ÇAYG7	ÇAYG8	ÇAYG9	**ÇAYG** SECTION
A	C	A	A	C	A	A	A	A	Total abundance
R	R	R	R	R	R	R	R	R	Total abundance of reworked forms
0.0	1.0	0.0	0.0	0.0	0.6	0.3	0.3	0.0	*Braarudosphaera* spp.
0.3	0.3	1.0	1.6	1.6	0.3	0.6	0.4	0.0	*Chiasmolithus* spp.
0.3	0.0	0.0	0.0	0.0	0.0	0.3	0.3	0.3	*Clausicoccus* spp.
5.0	3.3	4.0	3.6	4.0	1.6	1.3	1.0	6.3	*C. formosus*
3.3	5.0	3.7	3.6	4.6	1.3	3.3	2.6	10.3	*C. pelagicus*
74.0	67.0	43.0	58.0	51.0	66.1	52.0	59.0	54.0	*C. floridanus*
0.0	0.3	0.0	0.0	0.6	0.3	0.0	0.0	0.0	*Dictyococcites* sp.
0.3	0.0	0.0	0.0	0.3	0.0	0.0	0.3	0.3	*Helicosphaera* spp.
0.0	6.1	0.0	1.0	0.6	1.3	0.3	1.6	0.3	*L. minutus*
0.0	0.0	0.3	0.0	0.6	0.3	1.0	1.6	0.0	*Pemma* spp.
0.0	0.0	0.0	0.0	0.3	0.3	1.6	2.3	2.6	*P. inversus*
8.5	10.0	42.0	27.6	26.0	19.0	31.0	18.0	12.3	*R. dictyoda*
3.3	5.0	4.0	3.3	8.4	4.3	4.6	4.0	10.0	*Sphenolithus* spp.
5.0	2.0	2.0	1.3	2.0	4.6	3.7	8.6	3.6	*Z. bijugatus*
56.0	66.0	54.0	56.0	56.0	58.0	58.0	70.0	40.0	*Sphenolithus* sp.
0.0	0.0	0.0	0.0	0.0	0.0	0.0	4.0	20.0	*S. furcatolithoides*
0.0	cf	4.0	4.0	cf	cf	cf	4.0	4.0	*S. orphankollensis*
14.0	12.0	16.0	6.0	2.0	4.0	14.0	6.0	4.0	*S. perpendicularis*
4.0	2.0	8.0	8.0	6.0	4.0	4.0	0.0	14.0	*S. radians*
26.0	20.0	18.0	26.0	36.0	34.0	24.0	16.0	18.0	*S. spiniger*
0	0	1	0	0	0	1	0	0	*B. gladius*
9	10	1	2	3	7	1	9	0	*B. perampla*
1	2	2	0	0	0	1	9	0	*B. sequela*
2	0	1	1	1	1	0	1	0	*C. dela*
1	1	4	9	2	3	2	6	11	*C. grandis*
1	1	4	7	2	2	4	3	0	*C. nitidus+titus*
1	2	6	11	3	5	6	7	0	*C. solitus*
1	2	0	2	2	4	1	5	6	*Chiasmolithus* sp.
0	0	0	1	1	2	2	1	0	*C. gigas*
1	0	1	1	0	2	0	1	0	*C. mutatus*
0	0	1	1	0	0	0	0	0	*C. opdikey*
18	7	6	3	1	7	10	12	10	*D. barbadiensis*
0	0	0	0	0	0	0	0	2	*D. binodosus*
2	0	6	3	8	3	5	2	3	*D. deflandrei*
1	0	0	0	0	1	0	0	0	*D. kuepperi*
0	0	0	1	0	0	0	0	0	*D. nonaradiatus*
4	2	2	1	1	3	7	4	0	*D. saipanensis*
0	0	0	0	0	0	cf	0	0	*D. spinescens*
0	0	1	0	1	1	2	0	1	*D. tanii*
2	2	2	3	2	2	2	2	3	*Discoaster* sp.
1	0	3	0	1	2	0	0	1	*H. lophota*
1	0	2	1	0	1	0	1	0	*H. seminulum*
1	0	1	0	1	1	0	1	0	*Micrantholithus*
0	0	1	1	0	0	0	0	0	*N. alata/fulgens*
1	3	2	0	0	0	0	0	9	*N. cristata*
3	2	3	2	0	0	0	13	0	*Pemma* spp.
1	1	2	1	0	0	1	5	0	*P. versa*
0	2	0	0	0	1	0	0	0	*U. protoannulus*
CNE9-NP15p.p.-CP13a		CNE10-NP15p.p.-CP13bp.p.							Zone
Lutetian-middle Eocene									Age

Numbers in %

Numbers in %

Numbers on 100 FOV

Table S8. Quantitative distribution of calcareous nannofossils in the section ÇAYH.

ÇAYH1	ÇAYH2	ÇAYH3	ÇAYH4	ÇAYH5	ÇAYH6	ÇAYH7	ÇAYH8	**ÇAYH** SECTION
A	A	A	A	A	A	A	A	Total abundance
/	/	/	/	/	/	/	/	Total abundance of reworked forms
Numbers in %								
1.0	2.0	1.0	1.0	0.6	1.9	0.0	0.0	*Chiasmolithus* spp.
2.0	0.6	0.6	0.0	1.0	0.6	0.0	0.0	*Clausicoccus* spp.
8.0	11.3	8.0	15.0	9.0	8.0	10.0	8.3	*C. formosus*
19.0	8.0	10.0	9.0	9.0	9.0	12.0	11.0	*C. pelagicus*
37.0	47.0	40.0	38.0	50.0	45.0	52.0	38.0	*C. floridanus*
1.3	0.6	2.0	0.6	0.6	0.0	0.3	0.3	*Dictyococcites* sp.
3.0	0.9	0.0	1.6	0.3	0.0	2.3	3.3	*Discoaster* spp.
0.0	0.0	0.0	0.6	0.0	0.6	0.0	0.6	*Helicosphaera* spp.
1.6	1.6	2.3	3.0	1.6	3.6	1.0	1.3	*L. minutus*
1.3	0.6	1.0	0.6	1.0	1.0	0.0	1.0	*P. inversus*
9.6	10.0	18.3	11.0	10.3	13.0	10.3	22.0	*R. dictyoda+R. hillae*
15.0	13.0	16.0	18.3	13.0	14.0	10.6	11.0	*Sphenolithus* spp.
1.3	4.3	1.0	1.3	3.6	3.3	1.6	3.3	*Z. bijugatus*
62.0	54.0	42.0	70.0	52.0	68.0	88.0	76.0	*Sphenolithus* sp.
1.0	0.0	0.0	0.0	8.0	6.0	2.0	0.0	*S. cf cuniculus*
21.0	36.0	34.0	16.0	16.0	6.0	14.0	12.0	*S. furcatolithoides*
1.0	8.0	4.0	4.0	0.0	4.0	0.0	2.0	*S. radians*
15.0	2.0	20.0	10.0	24.0	16.0	6.0	10.0	*S. spiniger*
Numbers on 100 FOV								
6	2	1	0	0	1	2	0	*C. fenestratus*
14	8	5	5	10	7	8	6	*C. grandis*
0	2	1	0	2	3	0	0	*C. nitidus+titus*
4	5	3	2	7	3	1	1	*C. solitus*
14	4	6	7	5	3	4	2	*Chiasmolithus* sp.
cf	0	cf	0	cf	0	0	0	*C. gigas*
cf	0	2	1	3	2	1	0	*C. mutatus*
0	1	0	1	0	0	0	0	*C. opdikey*
8	6	6	13	4	4	17	20	*D. barbadiensis*
0	1	0	0	0	0	2	2	*D. bifax*
4	4	2	0	0	0	4	0	*D. deflandrei*
0	0	1	0	1	0	1	1	*D. nodifer*
9	11	2	8	5	4	4	1	*D. nonaradiatus*
3	2	0	2	0	2	1	2	*D. saipanensis*
1	0	0	0	0	0	0	1	*D. tanii*
18	14	7	14	6	0	19	13	*Discoaster* sp.
2	0	0	2	0	1	0	1	*H. lophota*
0	0	1	0	0	0	0	1	*H. seminulum*
0	0	0	2	2	2	2	1	*N. alata/fulgens*
4	2	4	1	7	3	1	0	*N. cristata*
1	0	0	0	0	0	2	1	*R. umbilicus*
CNE12-NP15p.p.-CP13c								Zone
Lutetian-middle Eocene								Age

Taxonomic list
Blackites Hay & Towe, 1962
Blackites gladius (Locker, 1967) Varol, 1989
Braarudosphaera Deflandre, 1947
Braarudosphaera perampla Bown, 2010
Braarudosphaera sequela Self-Trail, 2011
Campylosphaera Kamptner, 1963
Campylosphaera dela (Bramlette & Sullivan, 1961) Hay & Mohler, 1967
Chiasmolithus Hay et al., 1966
Chiasmolithus grandis (Bramlette & Riedel, 1954) Radomski, 1968
Chiasmolithus nitidus Perch-Nielsen, 1971
Chiasmolithus solitus (Bramlette & Sullivan, 1961) Locker, 1968
Chiasmolithus titus Gartner, 1970
Chiphragmalithus Bramlette & Sullivan, 1961
Clausicoccus Prins, 1979
Clausicoccus fenestratus (Deflandre & Fert, 1954) Prins, 1979
Clausicoccus subdistichus (Roth & Hay *in* Hay et al., 1967) Prins, 1979
Coccolithus Schwarz, 1894
Coccolithus crassus Bramlette & Sullivan, 1961
Coccolithus formosus (Kamptner, 1963) Wise, 1973
Coccolithus mutatus (Perch-Nielsen, 1971) Bown, 2005
Coccolithus opdykei Bown & Newsam, 2017
Coccolithus pelagicus (Wallich, 1877) Schiller, 1930
Cyclicargolithus Bukry 1971
Cyclicargolithus floridanus (Roth & Hay *in* Hay et al., 1967) Bukry, 1971
Dictyococcites Black, 1967
Discoaster Tan Sin Hok, 1927
Discoaster barbadiensis Tan Sin Hok, 1927
Discoaster bifax Bukry, 1971
Discoaster binodosus Martini, 1958
Discoaster deflandrei Bramlette & Riedel, 1954
Discoaster diastypus Bramlette & Sullivan, 1961
Discoaster gemmifer Stradner, 1961
Discoaster kuepperi Stradner, 1959
Discoaster lodoensis Bramlette & Riedel, 1954
Discoaster nodifer (Bramlette & Riedel, 1954) Bukry, 1973
Discoaster saipanensis Bramlette & Riedel, 1954
Discoaster septemradiatus (Klumpp, 1953) Martini, 1958
Discoaster sublodoensis Bramlette & Sullivan, 1961
Discoaster tanii Bramlette & Riedel, 1954
Ellipsolithus Sullivan, 1964
Ellipsolithus macellus (Bramlette & Sullivan, 1961) Sullivan, 1964
Helicosphaera Kamptner, 1954
Helicosphaera lophota (Bramlette & Sullivan, 1961) Locker, 1973
Helicosphaera seminulum Bramlette & Sullivan, 1961
Lanternithus Stradner, 1962
Lanternithus minutus Stradner, 1962
Micrantholithus Deflandre in Deflandre & Fert, 1954
Nannotetrina Achuthan & Stradner, 1969
Nannotetrina alata (Martini in Martini & Stradner, 1960) Haq & Lohmann, 1976
Nannotetrina cristata (Martini, 1958) Perch-Nielsen, 1971
Nannotetrina fulgens (Stradner in Martini & Stradner, 1960) Achuthan & Stradner, 1969
Pemma Klumpp, 1953
Pemma papillatum Martini, 1959
Pontosphaera Lohmann, 1902
Pontosphaera versa (Bramlette & Sullivan, 1961) Sherwood, 1974
Pseudotriquetrorhabdulus Wise in Wise & Constans, 1976
Pseudotriquetrorhabdulus inversus (Bukry & Bramlette, 1969) Wise in Wise & Constans, 1976
Reticulofenestra Hay, Mohler & Wade, 1966

Reticulofenestra dictyoda (Deflandre *in* Deflandre & Fert, 1954) Stradner *in* Stradner & Edwards, 1968
Reticulofenestra hillae Bukry & Percival, 1971
Reticulofenestra umbilicus (Levin, 1965) Martini & Ritzkowski, 1968
Sphenolithus Deflandre *in* Grassé, 1952
Sphenolithus cuniculus Bown, 2005
Sphenolithus editus Perch-Nielsen *in* Perch-Nielsen et al., 1978
Sphenolithus furcatolithoides Locker, 1967
Sphenolithus moriformis (Brönnimann & Stradner, 1960) Bramlette & Wilcoxon, 1967
Sphenolithus orphanknollensis Perch-Nielsen, 1971
Sphenolithus perpendicularis Shamrock, 2010
Sphenolithus primus Perch-Nielsen 1971
Sphenolithus radians Deflandre *in* Grassé, 1952
Sphenolithus spiniger Bukry, 1971
Sphenolithus villae Bown, 2005
Toweius gammation (Bramlette & Sullivan, 1961) Romein, 1979
Umbilicosphaera Lohmann, 1902
Umbilicosphaera protoannulus (Gartner, 1971) Young & Bown, 2014
Zygrhablithus Deflandre, 1959
Zygrhablithus bijugatus (Deflandre in Deflandre & Fert, 1954) Deflandre, 1959